

IRIS BASED HUMAN RECOGNITION SYSTEM

A Project Report

Submitted in fulfillment of the
requirement for the award of the degree of

Master of Computer Applications
(Session 2016 - 2017)

To



By

Name of the candidate

DUSHYANT KUMAR MEDHAVI (5142019)
SHIVANI RANA (5141010)
DINESH KUMAR (5142047)

Under the Supervision
of

Dr. Sarika Jain

DEPARTMENT OF COMPUTER APPLICATIONS
NATIONAL INSTITUTE OF TECHNOLOGY, KURUKSHETRA
November 2016

DECLARATION

We hereby declare that the work which is being presented in this project report entitled **“Iris Based Human Recognition System”**, in partial fulfillment of the requirement for the award of the degree of **MASTER OF COMPUTER APPLICATIONS** submitted to Department of Computer Applications, National Institute of Technology, Kurukshetra is an authentic work done by us during a period from to under the Guidance of

The work presented in this project report has not been submitted by us for the award of any other degree of this or any other Institute/University.

Dushyant Kumar Medhavi
5142019

Shivani Rana
5141010

Dinesh Kumar
5142047

This is to certify that the above statement made by the candidate is correct to best of my knowledge and belief.

Date:

Place:

Dr. Sarika Jain
Assistant Professor

ACKNOWLEDGEMENT

We would like to sincerely thank the National Institute of Technology Kurukshetra for giving us this opportunity of taking up such a challenging project which has enhanced our knowledge about the Image processing and to make a project on Iris Based Human Recognition System and how to make it easily available to users and clients of the agency.

We are very grateful to Dr Sarika Jain Project Supervisor, under whose guidance and assistance we were able to successfully complete our project. We are also thankful to Ms. Shashi Bala, Project Guide whose advice and thoughts helped us gain a better understanding of this huge huge concept of image processing.

Last but not the least; we also thank the below-mentioned honorable dignitaries and task-masters who have played a major role in our project to the sky of glory. This is a special thanks to them for sparing their precious time, fitting my out-of-the-way appointment into their diary and giving almost all the information required by us in an unbelievably amicable manner.

Without the priceless contribution and coveted guidance of all the above-mentioned people, this project would have never got a shape of reality and emerged before all of you in the manner and in the style as it now appears.

ABSTRACT

A biometric system provides automatic identification of an individual based on a unique feature or characteristic possessed by the individual. Iris recognition is regarded as the most reliable and accurate biometric identification system available. Most commercial iris recognition systems use patented algorithms developed by Daugman, and these algorithms are able to produce perfect recognition rates. However, published results have usually been produced under favourable conditions, and there have been no independent trials of the technology.

The work presented in this thesis involved developing an iris recognition system in order to verify both the uniqueness of the human iris and also its performance as a biometric. For determining the recognition performance of the system two databases of digitised greyscale eye images were used.

The iris recognition system consists of an automatic segmentation system that is based on the Hough transform, and is able to localize the circular iris and pupil region, occluding eyelids and eyelashes, and reflections. The extracted iris region was then normalised into a rectangular block with constant dimensions to account for imaging inconsistencies. Finally, the phase data from 1D Log-Gabor filters was extracted and quantized to four levels to encode the unique pattern of the iris into a bit-wise biometric template.

The Hamming distance was employed for classification of iris templates, and two templates were found to match if a test of statistical independence was failed. The system performed with perfect recognition on a set of 75 eye images; however, tests on another set of 624 images resulted in false accept and false reject rates of 0.005% and 0.238% respectively. Therefore, iris recognition is shown to be a reliable and accurate biometric technology.

LIST OF FIGURES

Figure No.	Figure Caption	Page No.
1.1	A front-on view of the human eye	2
2.1	Biometric Market in 2015	8
3.1	Stages of segmentation with eye image	13
3.2	Segmentation with eye image‘Pi201b From LET Dataset	16
3.3	Segmentation Fails for LET Data Set	17
3.4	The eyelash detection technique	17
3.5	segmentation of various images from the CASIA Data Set	18
3.6	segmentation of various images from the LET Data Set	18
4.1	Daugman’s Rubber Sheet Model	19
4.2	normalization process with radial resolution of 10 pixels	22
4.3	Illustration of the normalization process for two images	23
5.1	A quadrature pair of 2D Gabor filters	25
5.2	An illustration of the feature encoding process	30
5.3	An illustration of the shifting process	32
6.1	Input Dataset (CASIA)	34
6.2	Output of Localization Process	34
6.3	Normalize image with Noisy Part	35
6.4	Normalize image without Noisy Part	35
6.5	Enhancement of Normalize image	35

LIST OF TABLES

Table No.	Table Caption	Page No.
1.1	Bio-metric device Comparison based on properties	10
1.2	Bio-metric device Comparison based on Evaluation	14
5.2	Technical Specifications	24

TABLE OF CONTENTS

<i>Declaration</i>	i
<i>Acknowledgement</i>	ii
<i>Abstract.....</i>	iii
<i>List of Figure.....</i>	iv
<i>List of Tables</i>	v
<i>Table of Contents</i>	vi
 CHAPTER 1 INTRODUCTION	1
1.1 BIOMETRIC TECHNOLOGY	1
1.2 THE HUMAN IRIS	1
1.3 IRIS RECOGNITION	2
1.4 OBJECTIVE	3
 CHAPTER 2 LITERATURE REVIEW	4
2.1 OVERVIEW OF BIOMETRICS	4
2.1.1 Fingerprint recognition	4
2.1.2 Facial Recognition	5
2.1.3 Voice Recognition	6
2.1.4 Retina Scan	6
2.1.5 Hand Geometry	7
2.1.4 Iris Recognition	7
2.3 COMPARATIVE STUDY.....	8
2.4 RESEARCH GAP.....	10
 CHAPTER 3 SEGMENTATION.....	12
3.1 OVERVIEW	12
3.2 LITERATURE REVIEW.....	12
3.2.1 Hough Transform.....	12
3.2.2 Daugman's Integro-differential Operator	13
3.2.3 Active Contour Models	14
3.2.4 Eyelash and Noise Detection	14
3.3 IMPLEMENTATION.....	15
3.4 RESULTS	16
 CHAPTER 4 NORMALIZATION	19
4.1 OVERVIEW	19
4.2 LITERATURE REVIEW.....	19
4.2.1 Daugman's Rubber Sheet Model	19
4.2.2 Image Registration.....	20
4.2.3 Virtual Circles.....	21

4.3 IMPLEMENTATION	21
4.4 RESULTS	22
CHAPTER 5 FEATURE ENCODING AND MATCHING	24
5.1 OVERVIEW	24
5.2 LITERATURE REVIEW OF FEATURE ENCODING ALGORITHMS	24
5.2.1 <i>Wavelet Encoding</i>	24
5.2.2 <i>Gabor Filters</i>	24
5.2.3 <i>Log-Gabor Filters</i>	26
5.2.4 <i>Zero-crossings of the 1D wavelet</i>	26
5.2.5 <i>Haar Wavelet</i>	27
5.2.6 <i>Laplacian of Gaussian Filters</i>	27
5.3 LITERATURE REVIEW OF MATCHING ALGORITHMS	27
5.3.1 <i>Hamming distance</i>	27
5.3.2 <i>Weighted Euclidean Distance</i>	28
5.3.3 <i>Normalised Correlation</i>	28
5.4 IMPLEMENTATION	29
5.4.1 <i>Feature Encoding</i>	29
5.4.2 <i>Matching</i>	31
CHAPTER 6 SYSTEM TESTING AND PERFORMANCE EVALUATION ...	33
6.1 OVERVIEW	33
6.2 TECHNICAL SPECIFICATIONS	33
6.3 SEGMENTATION TESTING	34
6.4 NORMALIZATION TESTING	35
CHAPTER 7 CONCLUSION AND FUTURE RECOMMENDATIONS	36
7.1 CONCLUSION	36
7.2 LIMITATION	36
7.3 FUTURE SCOPE	36
BIBLIOGRAPHY	37
APPENDIX A SYSTEM OVERVIEW	38
APPENDIX B DETAILED EXPERIMENTAL RESULTS	39

Chapter 1

Introduction

1.1 Biometric Technology

A biometric system provides automatic recognition of an individual based on some sort of unique feature or characteristic possessed by the individual. Biometric systems have been developed based on fingerprints, facial features, voice, hand geometry, handwriting, the retina [1], and the one presented in this thesis, the iris.

Biometric systems work by first capturing a sample of the feature, such as recording a digital sound signal for voice recognition, or taking a digital color image for face recognition. The sample is then transformed using some sort of mathematical function into a biometric template. The biometric template will provide a normalised, efficient and highly discriminating representation of the feature, which can then be objectively compared with other templates in order to determine identity. Most biometric systems allow two modes of operation. An enrolment mode for adding templates to a database, and an identification mode, where a template is created for an individual and then a match is searched for in the database of pre-enrolled templates.

A good biometric is characterized by use of a feature that is; highly unique – so that the chance of any two people having the same characteristic will be minimal, stable – so that the feature does not change over time, and be easily captured – in order to provide convenience to the user, and prevent misrepresentation of the feature.

1.2 The Human Iris

The iris is a thin circular diaphragm, which lies between the cornea and the lens of the human eye. A front-on view of the iris is shown in Figure 1.1. The iris is perforated close to its centre by a circular aperture known as the pupil. The function of the iris is to control the amount of light entering through the pupil, and this is done by the sphincter and the dilator muscles, which adjust the size of the pupil. The average diameter of the iris is 12 mm, and the pupil size can vary from 10% to 80% of the iris diameter [2].

The iris consists of a number of layers; the lowest is the epithelium layer, which contains dense pigmentation cells. The stromal layer lies above the epithelium layer, and contains blood vessels, pigment cells and the two iris muscles. The density of stromal pigmentation determines the color of the iris. The externally visible surface of the multi-layered iris contains two zones, which often differ in color [3]. An outer ciliary zone and an inner pupillary zone, and these two zones are divided by the collarette – which appears as a zigzag pattern.

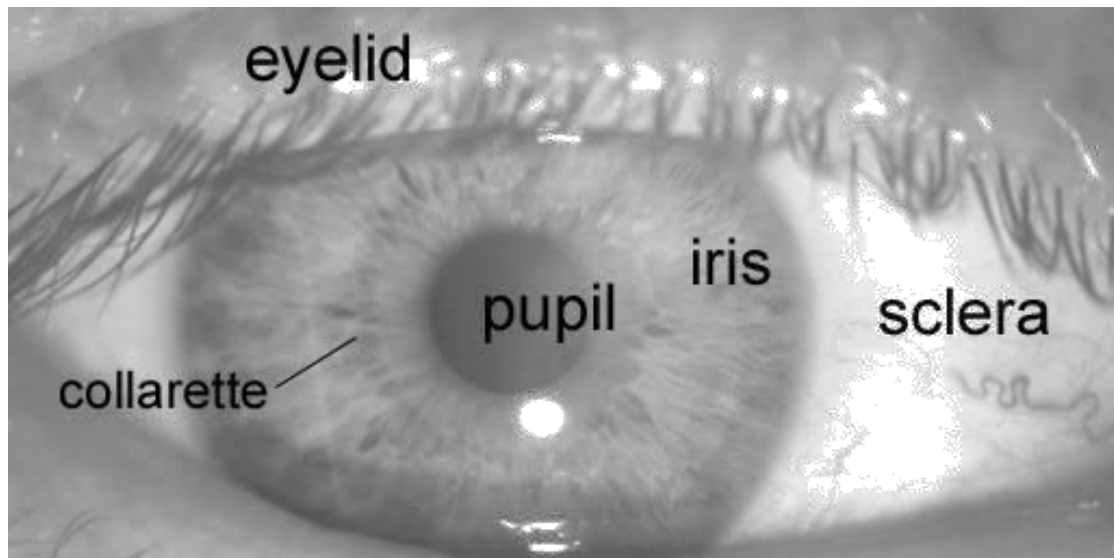


Figure 1.1 – A front-on view of the human eye.

Formation of the iris begins during the third month of embryonic life [3]. The unique pattern on the surface of the iris is formed during the first year of life, and pigmentation of the stroma takes place for the first few years. Formation of the unique patterns of the iris is random and not related to any genetic factors [4]. The only characteristic that is dependent on genetics is the pigmentation of the iris, which determines its color. Due to the epigenetic nature of iris patterns, the two eyes of an individual contain completely independent iris patterns, and identical twins possess uncorrelated iris patterns. For further details on the anatomy of the human eye consult the book by Wolff [3].

1.3 Iris Recognition

The iris is an externally visible, yet protected organ whose unique epigenetic pattern remains stable throughout adult life. These characteristics make it very attractive for use as a biometric for identifying individuals. Image processing techniques can be employed to extract the unique iris pattern from a digitized image of the eye, and encode it into a biometric template, which can be stored in a database. This biometric template contains an objective mathematical representation of the unique information stored in the iris, and allows comparisons to be made between templates. When a subject wishes to be identified by iris recognition system, their eye is first photographed, and then a template created for their iris region. This template is then compared with the other templates stored in a database until either a matching template is found and the subject is identified, or no match is found and the subject remains unidentified.

Although prototype systems had been proposed earlier, it was not until the early nineties that Cambridge researcher, John Daugman, implemented a working automated iris recognition system [1][2]. The Daugman system is patented [5] and the rights are now owned by the company Iridian Technologies. Even though the Daugman system is the most successful and most well known, many other systems have been developed. The most notable include the systems of Wildes et al. [7][4],

Boles and Boashash [8], Lim et al. [9], and Noh et al. [10]. The algorithms by Lim et al. are used in the iris recognition system developed by the Evermedia and Senex companies. Also, the Noh et al. algorithm is used in the 'IRIS2000' system, sold by IriTech. These are, apart from the Daugman system, the only other known commercial implementations.

The Daugman system has been tested under numerous studies, all reporting a zero failure rate. The Daugman system is claimed to be able to perfectly identify an individual, given millions of possibilities. The prototype system by Wildes et al. also reports flawless performance with 520 iris images [7], and the Lim et al. system attains a recognition rate of 98.4% with a database of around 6,000 eye images.

Compared with other biometric technologies, such as face, speech and finger recognition, iris recognition can easily be considered as the most reliable form of biometric technology [1]. However, there have been no independent trials of the technology, and source code for systems is not available. Also, there is a lack of publicly available datasets for testing and research, and the test results published have usually been produced using carefully imaged irises under favorable conditions.

1.4 Objective

The objective will be to implement an open-source iris recognition system in order to verify the claimed performance of the technology. The development tool used will be MATLAB[®] and emphasis will be only on the software for performing recognition, and not hardware for capturing an eye image. A rapid application development (RAD) approach will be employed in order to produce results quickly. MATLAB[®] provides an excellent RAD environment, with its image processing toolbox, and high level programming methodology. To test the system, two data sets of eye images will be used as inputs; a database of 756 greyscale eye images courtesy of The Chinese Academy of Sciences – Institute of Automation (CASIA) [13], and a database of 120 digital greyscale images courtesy of the Lion's Eye Institute (LEI) [14].

The system is to be composed of a number of sub-systems, which correspond to each stage of iris recognition. These stages are segmentation – locating the iris region in an eye image, normalization – creating a dimensionally consistent representation of the iris region, and feature encoding – creating a template containing only the most discriminating features of the iris. The input to the system will be an eye image, and the output will be an iris template, which will provide a mathematical representation of the iris region. For an overview of the components of the system see Appendix B.

Chapter 2

LITERATURE REVIEW

2.1 OVERVIEW OF BIOMETRICS

Recently biometric recognition has caused the researcher's great interest because of its many applications in the field of border control, surveillance, law enforcement, and national security. The primary aim of a biometric identification system is to recognize the identity of the target person on the basis of his/her physiological or behavioral characteristics. Examples of these characteristics include fingerprint, face, voice, signature, hand geometry, iris and palm print [1].

Authentication and security of individuals are necessary for many different areas the daily life, most people having daily to authenticate their identity; which include secure access to buildings, international travel, even something as common as an ATM. Biometric identification provides a valid alternative to traditional authentication mechanisms such as passwords and ID cards, while surmounting many problems of these methods; it is possible to identify a person based on "who they are" rather than "what they have" or "what information they can retain", for example passwords [2].

Ancient Egyptians used biometric system by measuring people to identify them. Biometrics refers to methods for distinctively recognizing individuals based on one or 2 more intrinsic physical or behavioral character. A biometric system provides automatic recognition of a person based on some of distinctive characteristics possessed by the individual.

Biometric systems have been developed based on the retina, facial features, voice, hand geometry, fingerprints, palm print, and the one presented in this report, the iris [3].

2.1.1 Fingerprint recognition

Fingerprint recognition or fingerprint authentication refers to the automated Method of verifying a match between two human fingerprints. The fingerprint is scanned electronically and a reference template created accordingly. This template may be derived from either minutiae element, the pattern of the fingerprint, or simply the image of the fingerprint. The inside surfaces of the hands and feet of all primates contain minute ridges of skin, with furrows between each ridge. The purpose of this skin structure is to facilitate exudation of perspiration, enhance sense of touch, and provide a gripping surface. Fingerprints are part of an individual's phenotype and hence are only weakly determined by genetics. Fingerprint is a pattern of ridges and valleys on the surface of the Fingerprint.

Many novel techniques have been developed over the last decade to acquire fingerprints without the use of ink. The basic principle of the ink-less methods is to sense the ridges on a finger, which are in contact with the surface of the scanner. The acquired image is called a "live scan" and the scanners are known as "livescan" fingerprint scanners .

There are three types of matching techniques:

- a. *Minutiae-based techniques*: In these minutiae points are found and then mapped to their relative position on finger. There are some difficulties like if image is of low quality it is difficult to find minutiae points correctly. Also it considers local position of ridges and furrows not global [23].
- b. *Correlation-based method*: It uses richer gray scale information. It overcome problems of above method, it can work with bad quality data. But it has some of its own problems like localization of points.
- c. *Pattern based (image based) matching*: Pattern based algorithms compare the basic fingerprint patterns (arch, whorl, and loop) between a stored template and a candidate fingerprint.

Advantages:

- ☐ It is the most developed method till now
- ☐ Relative inexpensive
- ☐ Even twins have unique fingerprint patterns so highly secure
- ☐ Small template size so matching is also fast

Applications:

- ☐ Verification on driver-license authenticity and license validity check
- ☐ Law Enforcement Forensics
- ☐ Border Control/Visa Issuance

2.1.2 Facial Recognition

Face recognition is based on both the shape and location of the eyes, eyebrows, nose, lips and chin. It is non intrusive method and very popular also. Facial recognition is carried out in two ways:

a. Facial metric: In this location and shape of facial attributes (e.g. distances between pupils or from nose to lip or chin) are measured.

b. Eigen faces: Analyzing the overall face image as “a weighted combination of a number of canonical faces.” Another emerging technique is to use face recognition combining with other visual details of skin. This technique is called as skin texture analysis. The unique lines, patterns, and spots apparent in a person’s skin is located. According to tests with this addition, performance in recognizing faces can increase 20 to 25 percent.

Advantages:

- ☐ Totally non intrusive
- ☐ Easy to store Templates
- ☐ Access Control

Applications:

- ☐ General identity verification
- ☐ Surveillance
- ☐ Access Control

2.1.3 Voice Recognition

It focuses on the vocal features that produce speech and not on the sound or the pronunciation of Speech. The vocal properties depend on the dimensions of the vocal tract, mouth, nasal cavities and the other speech processing mechanism of the human body. There are three different techniques.

- a. Text-dependent systems: The user is requested to speak a word or phrase which was earlier during the enrollment process. It is matched with stored pattern.
- b. Text-prompted systems: The user is prompted to repeat or read a word or phrase from a pre-recorded vocabulary Displayed by the system (e.g., *“Please say the numbers 7 8 3 4!”*).
- c. Text-independent systems: Systems have no initial knowledge /vocabulary. Reference templates are generated for different phonetic sounds of the human voice, rather than samples for certain words.

Advantages:

- ☐ Reliable
- ☐ Inexpensive
- ☐ Easy to use and no special instructions required

Applications:

- ☐ Robotics
- ☐ Automatic Translation
- ☐ Interactive voice response

2.1.4 Retina Scan

The blood vessels at the back of the eye have a unique pattern, from eye to eye and person to person. A light source is needed because retina is not visible. The infrared energy is absorbed faster by blood vessels in the retina than by the surrounding tissue. Based on this pattern of blood vessels can be easily recognized. It is required that a person remove its glasses, focus on a specific point for about 10-15 seconds. A coupler is used to read the blood vessel patterns. A coherent light source is also required for illumination [10].

Advantages:

- ☐ Retinal Scan can't be forged
- ☐ Error rate is 1 out of 10,000,000(almost 0%)
- ☐ Highly reliable

Applications:

- ☐ Utilized by several government agencies including the FBI, CIA, and NASA
- ☐ Used for medical diagnostic application

2.1.5 Hand Geometry

This recognition includes Measuring length, width, thickness and surface area, overall bone structure of the hand. The fact is that a person's hand is unique and it does not Change after certain age. Hand based system are of two types:

- a. Contact based:** a hand is placed on a reader's covered flat surface. This placement is positioned by five guides or pins that correctly situate the hand for the cameras.
- b. Contact-less based:** In this approach neither pegs nor platform are required for hand image acquisition.

Advantages:

- ☐ High reliable and accuracy.
- ☐ Robust, user friendly.
- ☐ Environmental factor, such as, dry weather that causes the drying of the skin is not an issue.

Applications:

- ☐ Majority of the nuclear power plants in the U.S. use hand recognition geometry for Access control.
- ☐ Used during 1996 Olympic Games.

2.1.4 Iris Recognition

The iris is the elastic, pigmented, connective tissue that controls the pupil. The iris is formed in early life in a process called morphogenesis. Once fully formed, the texture is stable throughout life. It is the most correct biometric recognition system so it is called as king of biometrics. The iris of the eye has a unique pattern, from eye to eye and person to person. Eye color is the color of iris. Iris recognition uses camera technology with subtle infrared illumination to acquire images of the detail-rich, intricate structures of the iris.

Advantages:

- ☐ Highly accurate.
- ☐ Highly scalable as iris structure remains same throughout lifetime.
- ☐ Small template size so fast matching.

Applications:

- ☐ All of the UAE's land, air and sea ports of entry are equipped with system.
- ☐ Adhaar card also has taken iris trait for recognition.
- ☐ Google uses iris scanners to control access to their datacenters.

2.3 Comparative Study

This Report is to provide the comparative study about various biometrics devices for authentication system .With the help of comparative study we can justify that which biometric device is best for security system.

A. Comparison based on biometric market

Mostly face, fingerprint, iris and AFIS are used in market and hand geometry is used in lowest no of applications. The complete pie chart is shown below:-

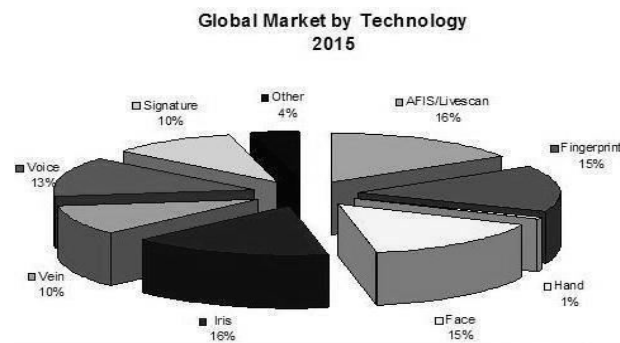


Fig.2.1 Biometric market in 2015

Iris recognition has the smallest outlier group of all biometric technologies, it is well-suited for one-to-many identification because of its speed of comparison and template longevity is a key advantage of this technology.

B. Based on properties

- ☐ *Universality*: Most of the population should have this trait.
- ☐ *Uniqueness*: Trait should be able to distinguish individuals.
- ☐ *Collectability*: The ease with which the data can be captured.
- ☐ *Permanence*: It should be almost constant for long run of time.
- ☐ *Performance*: How well the trait performs. It includes speed & security.
- ☐ *Acceptability*: To what extent people are willing to support this.
- ☐ *Circumvention*: Can this trait be cheated.

Biometric	Universality	Uniqueness	Collectability	Permanence	Performance	Acceptability	Circumvention
Fingerprint	M	H	M	M	M	H	M
Face	H	M	H	M	L	H	H
Iris	H	H	H	H	H	M	L
Retina	H	H	M	H	H	L	L
Hand Geometry	H	M	H	L	M	M	M
Voice	M	H	M	L	M	H	H

Table 1.1. Comparison based on properties

C. Comparison based on evaluation

There are various techniques based on which various modalities can be compared. These include false acceptance rate, false non acceptance rate, crossover error rate, failure to enroll rate, failure to capture rate, receiver capture characteristics, sensor subject distance etc.

- *FAR*: It refers to a situation where an unauthorized user is accepted by the authentication biometric machine as an authenticated person.
- *FRR*: It refers to a situation where an authorized person is rejected by the authentication biometric machine as an unauthenticated person.
- *CER*: The error rate at which FAR equals FRR. The minimum cross error rate, the more accurate and reliable the authentication biometric machine.
- *FTE*: The rate at which attempts to create a template from an input is unsuccessful.
- *FCR*: Within automatic systems, the probability that the system fails to detect a biometric input when presented correctly.
- *SSD*: The distance between human biometric part and biometric part reader device. It may vary as zero distance to several meters.

Biometric	FAR	FRR	Cross error	Failure to enroll rate	Failure to capture rate	Sensor subject distance
fingerprint	2%	2%	2%	1%	-	30cm
Face	1%	20%	-	NA	NA	20m
Iris	0.94%	0.99%	0.01%	0.5%	-	30CM
Retina	0.91%	0.04%	0.8%	-	-	30CM
Hand Geometry	2%	2%	1%	NA	NA	10CM
Voice	2%	10%	6%	-	-	20CM

Table 1.2. Based On Evaluation

2.4 Research Gaps

Fingerprint Recognition:-

- ☐ The recognition rate of finger print based biometric recognition system degrades greatly when the finger is wet and wrinkled. The impact of wet and wrinkled finger on biometric system performance has not been well addressed yet.
- ☐ Elastic distortion of the skin of the finger due to touch sensing methods and potential problems with cleanliness of the sensor and public hygiene.
- ☐ Cuts, scars can produce obstacle for recognition.
- ☐ The security systems can be cheated by having artificial finger like finger made up of wax.

Face Recognition:-

- ☐ The main drawbacks to face recognition are its current relatively low accuracy (compared to the proven performance of fingerprint and iris recognition) and less effective if facial expressions vary.
- ☐ Even a big smile can render the system less effective.
- ☐ Two facial appearance Factors effected-Intrinsic Factors AND Extrinsic Factors.
- ☐ Intrinsic factors are due purely to the physical nature of the face and are independent of the observer. These factors can be intrapersonal Factors .
- ☐ Intrapersonal factors are responsible for varying the facial appearance of the same person, some examples being age, facial expression and facial paraphernalia (facial hair, glasses, cosmetics, etc.).

Voice Recognition:-

- ☐ Affected by noisy environment
- ☐ Very large database
- ☐ Changes if person suffering from cold
- ☐ Depend on emotional condition of individuals

Retina Scan:-

- ☐ Reveals some medical conditions (e.g. hypertension), which causes privacy issues
- ☐ It is intrusive so not user friendly
- ☐ measurement accuracy can be affected by a disease such as cataracts

Hand Geometry:-

- ☐ The hand geometry is not unique and cannot be used in identification systems
- ☐ Not ideal for growing children
- ☐ Jewelry (rings, etc), limited dexterity (arthritis, etc) etc may pose a challenge

Iris Recognition:-

- ☐ It is the most correct bio-metric recognition system so it is called as king of biometrics but in spite of these features iris recognition deals with some challenges:-
 - ☐ The recognition rate degrades if eyes are covered by some occlusions.
 - ☐ Research in this area seeks more effort to assure its reliability against several factors such as contact lenses, eye glasses, watery eyes etc.
 - ☐ Iris scanners are relatively expensive.
 - ☐ The iris biometric is not left as evidence on crime scene so it is not useful for forensic applications.

Chapter 3

SEGMENTATION

3.1 Overview

The first stage of iris recognition is to isolate the actual iris region in a digital eye image. The iris region, shown in Figure 1.1, can be approximated by two circles, one for the iris/sclera boundary and another, interior to the first, for the iris/pupil boundary. The eyelids and eyelashes normally occlude the upper and lower parts of the iris region. Also, specular reflections can occur within the iris region corrupting the iris pattern. A technique is required to isolate and exclude these artefacts as well as locating the circular iris region.

The success of segmentation depends on the imaging quality of eye images. Images in the CASIA iris database [13] do not contain specular reflections due to the use of near infra- red light for illumination. However, the images in the LEI database [14] contain these specular reflections, which are caused by imaging under natural light. Also, persons with darkly pigmented irises will present very low contrast between the pupil and iris region if imaged under natural light, making segmentation more difficult. The segmentation stage is critical to the success of an iris recognition system, since data that is falsely represented as iris pattern data will corrupt the biometric templates generated, resulting in poor recognition rates.

3.2 *LITERATURE REVIEW*

3.2.1 Hough Transform

The Hough transform is a standard computer vision algorithm that can be used to determine the parameters of simple geometric objects, such as lines and circles, present in an image. The circular Hough transform can be employed to deduce the radius and centre coordinates of the pupil and iris regions. An automatic segmentation algorithm based on the circular Hough transform is employed by Wildes et al. [7], Kong and Zhang [15], Tisse et al. [12], and Ma et al. [16]. Firstly, an edge map is generated by calculating the first derivatives of intensity values in an eye image and then thresholding the result. From the edge map, votes are cast in Hough space for the parameters of circles passing through each edge point. These parameters are the centre Coordinates x_c and y_c , and the radius r , which are able to define any circle according to the equation

$$x_c^2 + y_c^2 - r^2 = 0 \quad (3.1)$$

A maximum point in the Hough space will correspond to the radius and centre coordinates of the circle best defined by the edge points. Wildes et al. and Kong and Zhang also make use of the parabolic Hough transform to detect the eyelids, approximating the upper and lower eyelids with parabolic arcs, which are represented as;

$$(-(x - h_j)\sin\theta_j + (y - k_j)\cos\theta_j)^2 = a_j((x - h_j)\cos\theta_j + (y - k_j)\sin\theta_j) \quad (2.2)$$

where a_j controls the curvature, (h_j, k_j) is the peak of the parabola and θ_j is the angle of rotation relative to the x-axis.

In performing the preceding edge detection step, Wildes et al. bias the derivatives in the horizontal direction for detecting the eyelids, and in the vertical direction for detecting the outer circular boundary of the iris, this is illustrated in Figure 2.1. The motivation for this is that the eyelids are usually horizontally aligned, and also the eyelid edge map will corrupt the circular iris boundary edge map if using all gradient data. Taking only the vertical gradients for locating the iris boundary will reduce influence of the eyelids when performing circular Hough transform, and not all of the edge pixels defining the circle are required for successful localization. Not only does this make circle localization more accurate, it also makes it more efficient, since there are less edge points to cast votes in the Hough space.

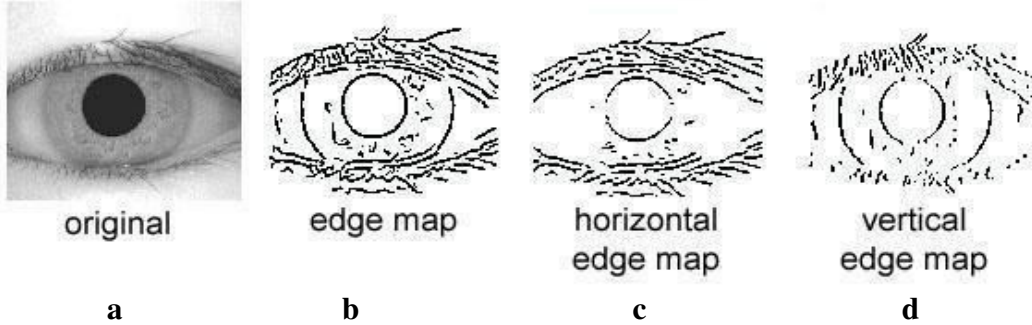


Figure 3.1– **a)** an eye image (020_2_1 from the CASIA database) **b)** corresponding edge map **c)** edge map with only horizontal gradients **d)** edge map with only vertical gradients.

There are a number of problems with the Hough transform method. First of all, it requires threshold values to be chosen for edge detection, and this may result in critical edge points being removed, resulting in failure to detect circles/arcs. Secondly, the Hough transform is computationally intensive due to its ‘brute-force’ approach, and thus may not be suitable for real time applications.

3.2.2 Daugman’s Integro-differential Operator

Daugman makes use of an Integro-differential operator for locating the circular iris and pupil regions, and also the arcs of the upper and lower eyelids. The Integro-differential operator is defined as

$$\max_{(r, x_p, y_p)} \left| -G_{\sigma}(r) * \frac{\partial}{\partial r} \right|_{r=x_0, y_0} I(x, y) \quad (3.3)$$

where $I(x, y)$ is the eye image, r is the radius to search for, $G_{\sigma}(r)$ is a Gaussian

Smoothing function and s is the contour of the circle given by r, x_0, y_0 . The operator searches for the circular path where there is maximum change in pixel values, by varying the radius and centre x and y position of the circular contour. The operator is applied iteratively with the amount of smoothing progressively reduced in order to attain precise localization. Eyelids are localized in a similar manner, with the path of contour integration changed from circular to an arc.

The Integro-differential can be seen as a variation of the Hough transform, since it too makes use of first derivatives of the image and performs a search to find geometric parameters. Since it works with raw derivative information, it does not suffer from the thresholding problems of the Hough transform. However, the algorithm can fail where there is noise in the eye image, such as from reflections, since it works only on a local scale.

3.2.3 Active Contour Models

Ritter et al. [17] make use of active contour models for localizing the pupil in eye images. Active contours respond to pre-set internal and external forces by deforming internally or moving across an image until equilibrium is reached. The contour contains a number of vertices, whose positions are changed by two opposing forces, an internal force, which is dependent on the desired characteristics, and an external force, which is dependent on the image. Each vertex is moved between time t and $t + 1$ by

$$v_i(t + 1) = v_i(t) + F_i(t) + G_i(t) \quad (3.4)$$

Where F_i is the internal force, G_i is the external force and v_i is the position of vertex i . For localization of the pupil region, the internal forces are calibrated so that the contour forms a globally expanding discrete circle. The external forces are usually found using the edge information. In order to improve accuracy Ritter et al. use the variance image, rather than the edge image.

A point interior to the pupil is located from a variance image and then a discrete circular active contour (DCAC) is created with this point as its centre. The DCAC is then moved under the influence of internal and external forces until it reaches equilibrium, and the pupil is localized.

3.2.4 Eyelash and Noise Detection

Kong and Zhang [15] present a method for eyelash detection, where eyelashes are treated as belonging to two types, separable eyelashes, which are isolated in the image, and multiple eyelashes, which are bunched together and overlap in the eye

image. Separable eyelashes are detected using 1D Gabor filters, since the convolution of a separable eyelash with the Gaussian smoothing function results in a low output value. Thus, if a resultant point is smaller than a threshold, it is noted that this point belongs to an eyelash. Multiple eyelashes are detected using the variance of intensity. If the variance of intensity values in a small window is lower than a threshold, the centre of the window is considered as a point in an eyelash. The Kong and Zhang model also makes use of connective criterion, so that each point in an eyelash should connect to another point in an eyelash or to an eyelid. Specular reflections along the eye image are detected using thresholding, since the intensity values at these regions will be higher than at any other regions in the image.

3.3 Implementation

It was decided to use circular Hough transform for detecting the iris and pupil boundaries. This involves first employing canny edge detection to generate an edge map. Gradients were biased in the vertical direction for the outer iris/sclera boundary, as suggested by Wildes et al. [4]. Vertical and horizontal gradients were weighted equally for the inner iris/pupil boundary. A modified version of Kovese's Canny edge Detection MATLAB[®] function [22] was implemented, which allowed for weighting of the gradients.

The range of radius values to search for was set manually, depending on the database used. For the CASIA database, values of the iris radius range from 90 to 150 pixels, while the pupil radius ranges from 28 to 75 pixels. In order to make the circle detection process more efficient and accurate, the Hough transform for the iris/sclera boundary was performed first, then the Hough transform for the iris/pupil boundary was performed within the iris region, instead of the whole eye region, since the pupil is always within the iris region. After this process was complete, six parameters are stored, the radius, and x and y centre coordinates for both circles.

Eyelids were isolated by first fitting a line to the upper and lower eyelid using the linear Hough transform. A second horizontal line is then drawn, which intersects with the first line at the iris edge that is closest to the pupil. This process is illustrated in Figure 2.2 and is done for both the top and bottom eyelids. The second horizontal line allows maximum isolation of eyelid regions. Canny edge detection is used to create an edge map, and only horizontal gradient information is taken. The linear Hough

Transform is implemented using the MATLAB[®] Radon transform, which is a form of the Hough transform. If the maximum in Hough space is lower than a set threshold, then no line is fitted, since this corresponds to non-occluding eyelids. Also, the lines are restricted to lie exterior to the pupil region, and interior to the iris region. A linear Hough transform has the advantage over its parabolic version, in that there are less parameters to deduce, making the process less computationally demanding.

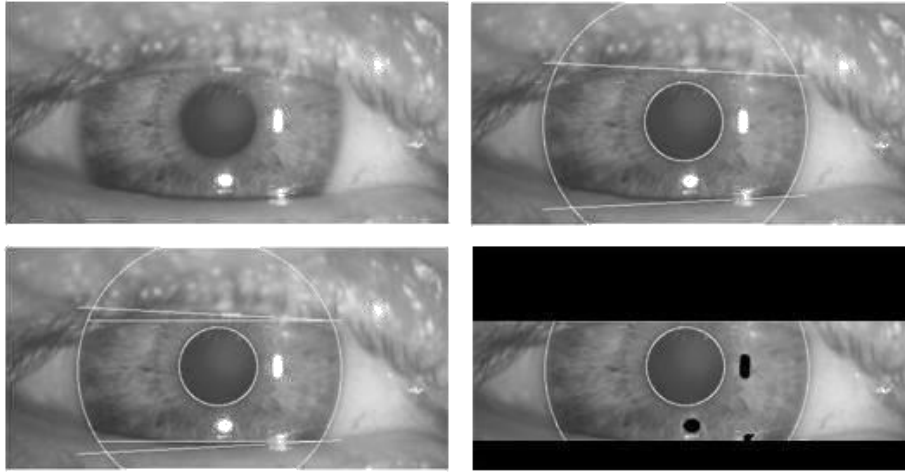


Figure 3.2 - Stages of segmentation with eye image ‘pi201b’ from the LEI database **Top left**) original eye image **Top right**) two circles overlaid for iris and pupil boundaries, and two lines for top and bottom eyelid **Bottom left**) horizontal lines are drawn for each eyelid from the lowest/highest point of the fitted line **Bottom right**) probable eyelid and specular reflection areas isolated (black areas)

For isolating eyelashes in the CASIA database a simple thresholding technique was used, since analysis reveals that eyelashes are quite dark when compared with the rest of the eye image. Analysis of the LEI eye images shows that thresholding to detect eyelashes would not be successful. Although, the eyelashes are quite dark compared with the surrounding eyelid region, areas of the iris region are equally dark due to the imaging conditions. Therefore thresholding to isolate eyelashes would also remove important iris region features, making this technique infeasible. However, eyelash occlusion is not very prominent so no technique was implemented to isolate eyelashes in the LEI database.

The LEI database also required isolation of specular reflections. This was implemented, again, using thresholding, since reflection areas are characterized by high pixel values close to 255. For the eyelid, eyelash, and reflection detection

Process, the coordinates of any of these noise areas are marked using the MATLAB[®] NaN type, so that intensity values at these points are not misrepresented as iris region data.

3.4 Results

The automatic segmentation model proved to be successful. The CASIA database provided good segmentation, since those eye images had been taken specifically for iris recognition research and boundaries of iris pupil and sclera were clearly distinguished. For the CASIA database, the segmentation technique managed to correctly segment the iris region from 624 out of 756 eye images, which corresponds to a success rate of around 83%. The LEI images proved problematic and the segmentation process correctly identified iris and pupil boundaries for only 75 out of 120 eye images, which corresponds to a success rate of around 62%.

The problem images had small intensity differences between the iris region and the pupil region as shown in Figure 2.3. One problem faced with the implementation was

that it required different parameters to be set for each database. These parameters were the radius of iris and pupil to search for, and threshold values for creating edge maps. However, for installations of iris recognition systems, these parameters would only need to be set once, since the camera hardware, imaging distance, and lighting conditions would usually remain the same.

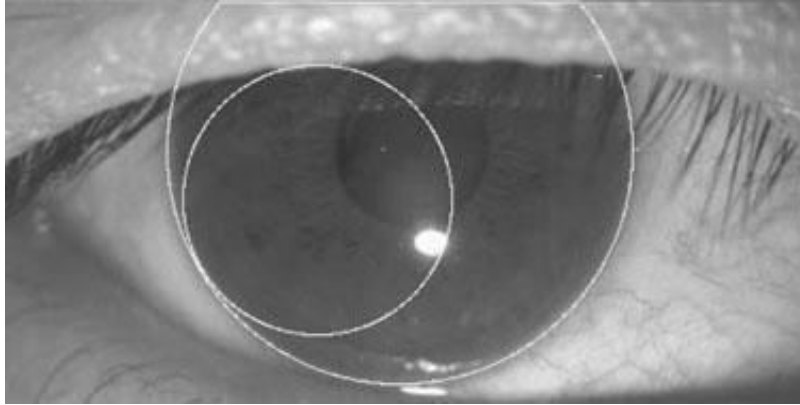


Figure 3.3 – An example where segmentation fails for the LEI database. Here there is little contrast between pupil and iris regions, so Canny edge detection fails to find the edges of the pupil border.

The eyelid detection system also proved quite successful, and managed to isolate most occluding eyelid regions. One problem was that it would sometimes isolate too much of the iris region, which could make the recognition process less accurate, since there is less iris information. However, this is preferred over including too much of the iris region, if there is a high chance it would also include undetected eyelash and eyelid regions.

The eyelash detection system implemented for the CASIA database also proved to be successful in isolating most of the eyelashes occurring within the iris region as shown in Figure 3.4.

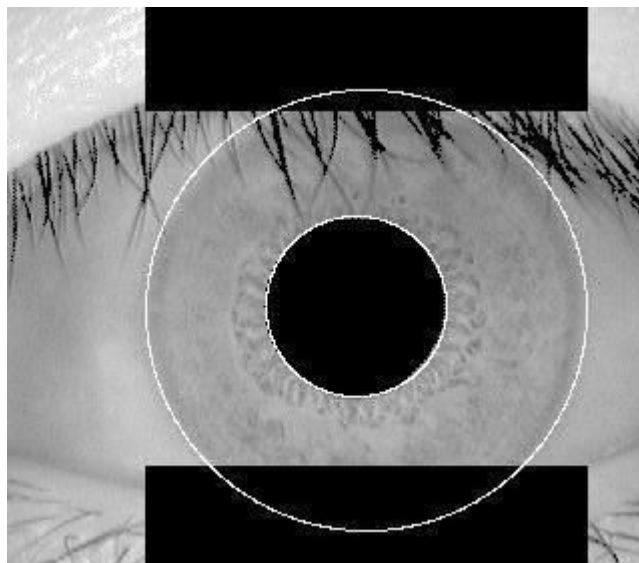


Figure 3.4 – The eyelash detection technique, eyelash regions are detected using thresholding and denoted as black. Note that some lighter eyelashes are not detected. Image ‘021_1_2’ from the CASIA database.

A slight problem was that areas where the eyelashes were light, such as at the tips, were not detected. However, these undetected areas were small when compared with the size of the iris region. Isolation of specular reflections from eye images in the LEI database also proved to be successful and numerous examples of their isolation are shown in Figure 3.6.

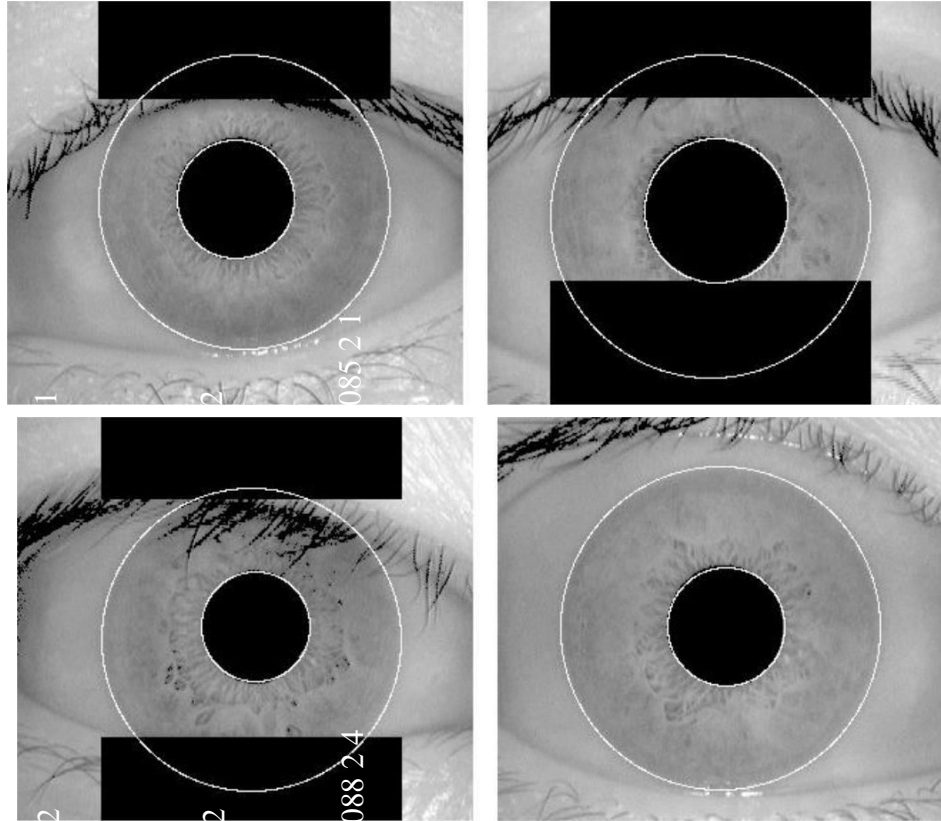


Figure 3.5 – Automatic segmentation of various images from the CASIA database. Black regions denote detected eyelid and eyelash regions.

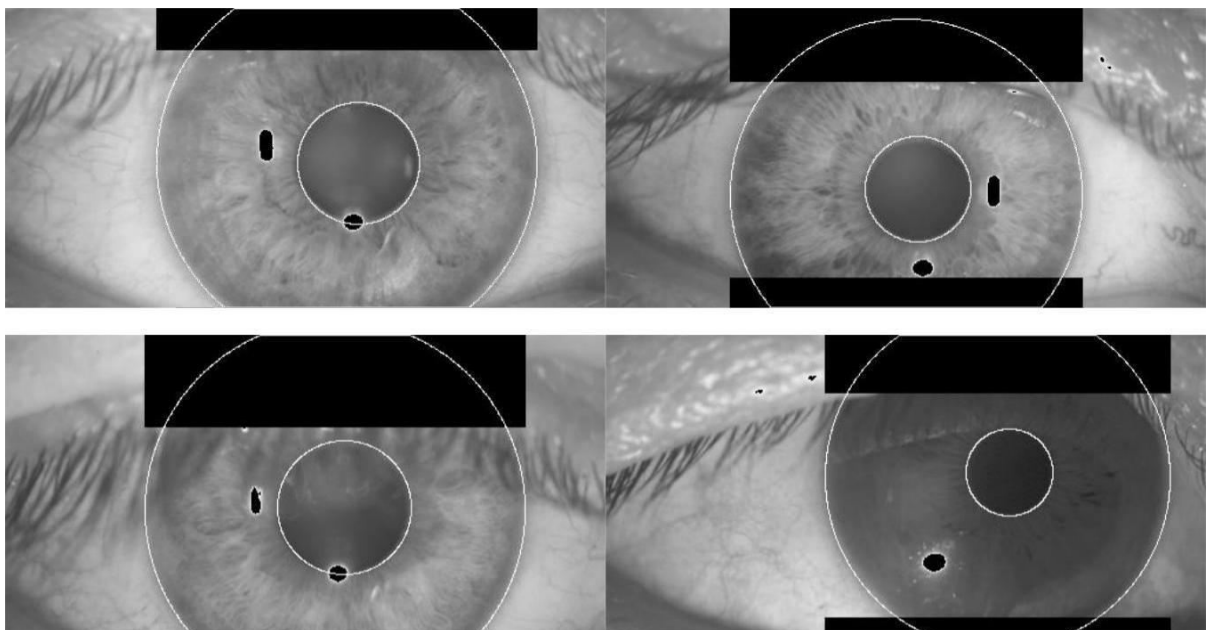


Figure 3.6 – Automatic segmentation of various images from the 'LEI' database, note the undetected occluding eyelashes in 'ra201b' and 'bo201c'. Black regions denote detected eyelids and specular reflections.

Chapter 4

Normalization

4.1 Overview

Once the iris region is successfully segmented from an eye image, the next stage is to transform the iris region so that it has fixed dimensions in order to allow comparisons. The dimensional inconsistencies between eye images are mainly due to the stretching of the iris caused by pupil dilation from varying levels of illumination. Other sources of inconsistency include, varying imaging distance, rotation of the camera, head tilt, and rotation of the eye within the eye socket. The normalization process will produce iris regions, which have the same constant dimensions, so that two photographs of the same iris under different conditions will have characteristic features at the same spatial location.

Another point of note is that the pupil region is not always concentric within the iris region, and is usually slightly nasal [2]. This must be taken into account if trying to normalize the ‘doughnut’ shaped iris region to have constant radius.

4.2 LITERATURE REVIEW

4.2.1 Daugman’s Rubber Sheet Model

The homogenous rubber sheet model devised by Daugman [1] remaps each point within the iris region to a pair of polar coordinates (r, θ) where r is on the interval $[0,1]$ and θ is angle $[0,2\pi]$.

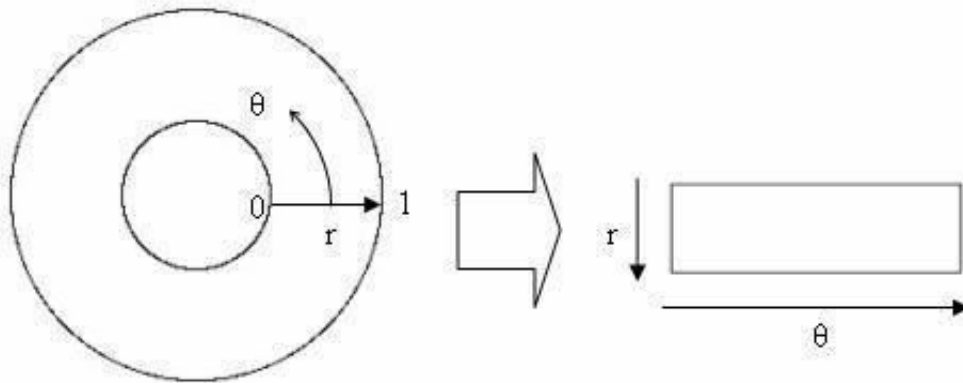


Figure 4.1 – Daugman’s rubber sheet model.

The remapping of the iris region from (x,y) Cartesian coordinates to the normalized non-concentric polar representation is modeled as

$$I(x(r,\theta), y(r,\theta)) \rightarrow I(r,\theta) \quad (4.1)$$

with

$$x(r,\theta) = (1-r)x_p(\theta) + rx_l(\theta)$$

$$y(r,\theta) = (1-r)y_p(\theta) + ry_l(\theta)$$

where $I(x,y)$ is the iris region image, (x,y) are the original Cartesian coordinates, (r,θ) are the corresponding normalised polar coordinates, and x_p, y_p and x_l, y_l are the coordinates of the pupil and iris boundaries along the θ direction. The rubber sheet model takes into account pupil dilation and size inconsistencies in order to produce a normalised representation with constant dimensions. In this way the iris region is modelled as a flexible rubber sheet anchored at the iris boundary with the pupil centre as the reference point.

Even though the homogenous rubber sheet model accounts for pupil dilation, imaging distance and non-concentric pupil displacement, it does not compensate for rotational inconsistencies. In the Daugman system, rotation is accounted for during matching by shifting the iris templates in the θ direction until two iris templates are aligned.

4.2.2 Image Registration

The Wildes et al. system employs an image registration technique, which geometrically warps a newly acquired image, $I_a(x, y)$ into alignment with a selected database image $I_d(x, y)$ [4]. When choosing a mapping function $(u(x, y), v(x, y))$ to transform the original coordinates, the image intensity values of the new image are made to be close to those of corresponding points in the reference image. The mapping function must be chosen so as to minimize

$$\int_x \int_y (I_d(x, y) - I_a(x - u, y - v))^2 dx dy \quad (4.2)$$

while being constrained to capture a similarity transformation of image coordinates (x, y) to (x', y') , that is

$$\begin{pmatrix} x' \\ y' \end{pmatrix} = \begin{pmatrix} x \\ y \end{pmatrix} - sR(\varphi) \quad (4.3)$$

with s a scaling factor and $R(\varphi)$ a matrix representing rotation by φ . In implementation, given a pair of iris images I_a and I_d , the warping parameters s and φ are recovered via an iterative minimization procedure [4].

4.2.3 Virtual Circles

In the Boles [8] system, iris images are first scaled to have constant diameter so that when comparing two images, one is considered as the reference image. This works differently to the other techniques, since normalization is not performed until attempting to match two iris regions, rather than performing normalization and saving the result for later comparisons. Once the two irises have the same dimensions, features are extracted from the iris region by storing the intensity values along virtual concentric circles, with origin at the centre of the pupil. A normalization resolution is Selected, so that the number of data points extracted from each iris is the same. This is **essentially the same as Daugman's rubber sheet model, however scaling** is at match Time, and is relative to the comparing iris region, rather than scaling to some constant dimensions. Also, it is not mentioned by Boles, how rotational invariance is obtained.

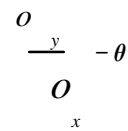
4.3 Implementation

For normalization of iris regions a technique based on Daugman's rubber sheet model was employed. The centre of the pupil was considered as the reference point, and radial vectors pass through the iris region, as shown in Figure 3.2. A number of data points are selected along each radial line and this is defined as the radial resolution. The number of radial lines going around the iris region is defined as the angular resolution. Since the pupil can be non-concentric to the iris, a remapping formula is needed to rescale points depending on the angle around the circle. This is given by

$$r' = \sqrt{\alpha} \beta \pm \sqrt{\alpha \beta^2 - \alpha - r^2} \quad (4.4)$$

with

$$\alpha = o_x^2 + o_y^2$$



where displacement of the centre of the pupil relative to the centre of the iris is given by o_x , o_y , and r' is the distance between the edge of the pupil and edge of the iris at an angle, θ around the region, and r is the radius of the iris. The remapping formula first gives the radius of the iris region 'doughnut' as a function of the angle θ .

A constant number of points are chosen along each radial line, so that a constant number of radial data points are taken, irrespective of how narrow or wide the radius is at a particular angle. The normalized pattern was created by backtracking to find the Cartesian coordinates of data points from the radial and angular position in the normalized pattern. From the 'doughnut' iris region, normalization produces a 2D array with horizontal dimensions of angular resolution and vertical dimensions of radial resolution. Another 2D array was created for marking reflections, eyelashes, and eyelids detected in the segmentation stage. In order to prevent non-iris region data from corrupting the normalized representation, data points which occur along the

pupil border or the iris border are discarded. As in Daugman's rubber sheet model, removing rotational inconsistencies is performed at the matching stage and will be discussed in the next chapter.

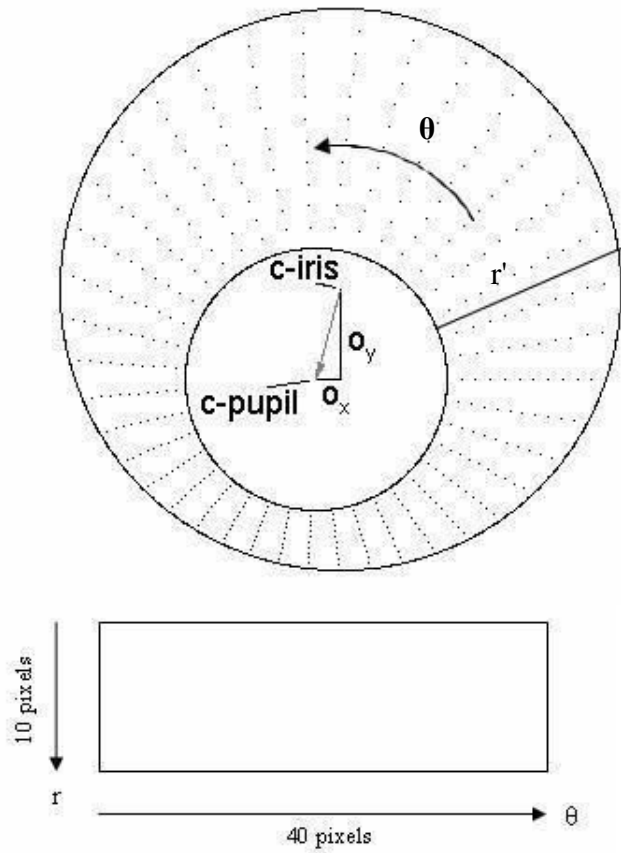


Figure 4.2 – Outline of the normalization process with radial resolution of 10 pixels, and angular resolution of 40 pixels. Pupil displacement relative to the iris centre is exaggerated for illustration purposes.

4.4 Results

The normalization process proved to be successful and some results are shown in Figure 3.3. However, the normalization process was not able to perfectly reconstruct the same pattern from images with varying amounts of pupil dilation, since deformation of the iris results in small changes of its surface patterns.

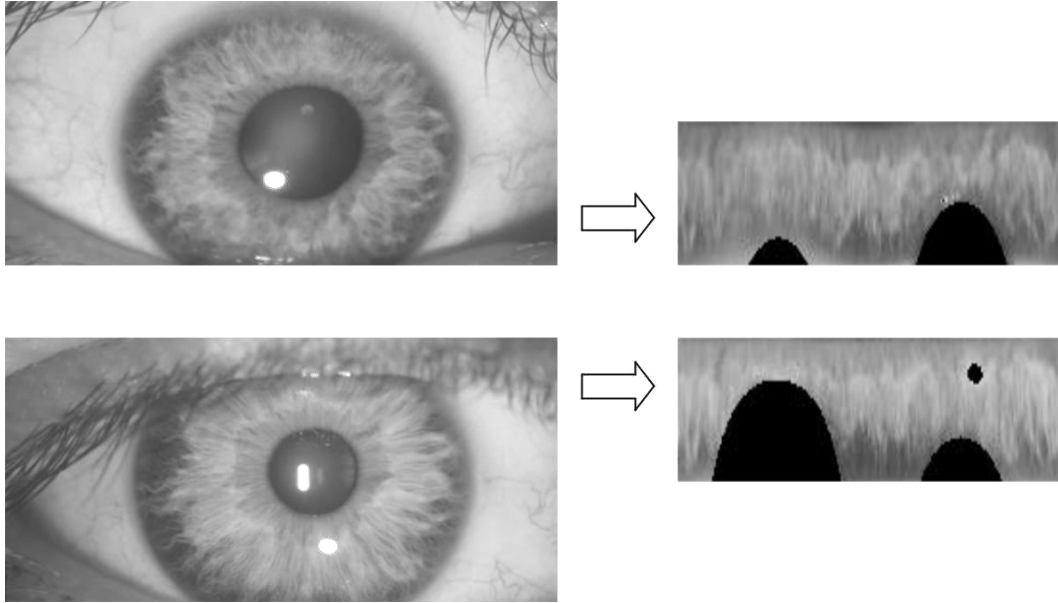


Figure 4.3 – Illustration of the normalization process for two images of the same iris taken under varying conditions. Top image ‘am201b’, bottom image ‘am201g’ from the LEI database.

Normalization of two eye images of the same iris is shown in Figure 3.3. The pupil is smaller in the bottom image, however the normalization process is able to rescale the iris region so that it has constant dimension. In this example, the rectangular representation is constructed from 10,000 data points in each iris region. Note that rotational inconsistencies have not been accounted for by the normalization process, and the two normalized patterns are slightly misaligned in the horizontal (angular) direction. Rotational inconsistencies will be accounted for in the matching stage.

Chapter 5

Feature Encoding and Matching

5.1 Overview

In order to provide accurate recognition of individuals, the most discriminating information present in an iris pattern must be extracted. Only the significant features of the iris must be encoded so that comparisons between templates can be made. Most iris recognition systems make use of a band pass decomposition of the iris image to create a biometric template.

The template that is generated in the feature encoding process will also need a corresponding matching metric, which gives a measure of similarity between two iris templates. This metric should give one range of values when comparing templates generated from the same eye, known as intra-class comparisons, and another range of values when comparing templates created from different irises, known as inter-class comparisons. These two cases should give distinct and separate values, so that a decision can be made with high confidence as to whether two templates are from the same iris, or from two different irises.

4.5 Literature Review of Feature Encoding Algorithms

5.2.1 Wavelet Encoding

Wavelets can be used to decompose the data in the iris region into components that appear at different resolutions. Wavelets have the advantage over traditional Fourier transform in that the frequency data is localized, allowing features which occur at the same position and resolution to be matched up. A number of wavelet filters, also called a bank of wavelets, is applied to the 2D iris region, one for each resolution with each wavelet a scaled version of some basis function. The output of applying the wavelets is then encoded in order to provide a compact and discriminating representation of the iris pattern.

5.2.2 Gabor Filters

Gabor filters are able to provide optimum conjoint representation of a signal in space and spatial frequency. A Gabor filter is constructed by modulating a sine/cosine wave with a Gaussian. This is able to provide the optimum conjoint localisation in both space and frequency, since a sine wave is perfectly localised in frequency, but not localised in space. Modulation of the sine with a Gaussian provides localisation in space, though with loss of localisation in frequency. Decomposition of a signal is accomplished using a quadrature pair of Gabor filters, with a real part specified by a cosine modulated by a Gaussian, and an imaginary part specified by a sine modulated

by a Gaussian. The real and imaginary filters are also known as the even symmetric and odd symmetric components respectively.

The centre frequency of the filter is specified by the frequency of the sine/cosine wave, and the bandwidth of the filter is specified by the width of the Gaussian.

Daugman makes use of a 2D version of Gabor filters [1] in order to encode iris pattern data. A 2D Gabor filter over the an image domain (x,y) is represented as

$$G(x, y) = e^{-\pi[(x-x_0)^2/\alpha^2 + (y-y_0)^2/\beta^2]} e^{-2\pi i[u_0(x-x_0) + v_0(y-y_0)]} \quad (5.1)$$

where (x_0, y_0) specify position in the image, (α, β) specify the effective width and length, and (u_0, v_0) specify modulation, which has spatial frequency $\omega_0 = \sqrt{u_0^2 + v_0^2}$. The odd symmetric and even symmetric 2D Gabor filters are shown in Figure 4.1.

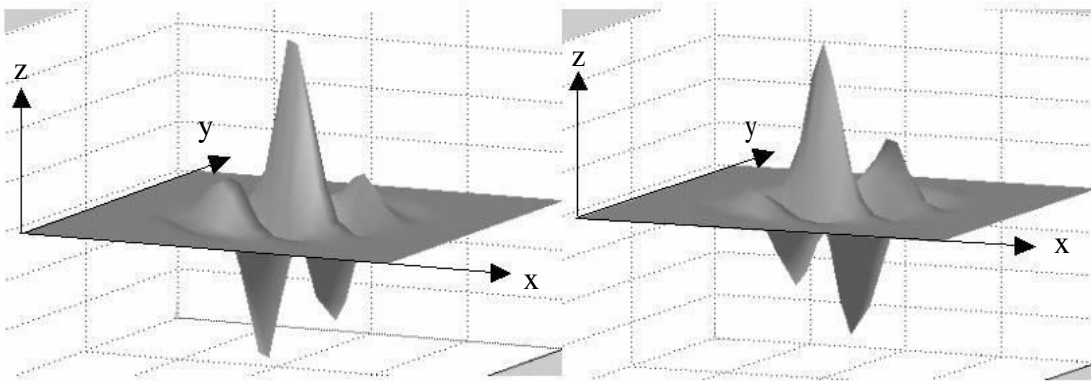


Figure 5.1 – A quadrature pair of 2D Gabor filters **left**) real component or even symmetric filter characterised by a cosine modulated by a Gaussian **right**) imaginary component or odd symmetric filter characterised by a sine modulated by a Gaussian.

Daugman demodulates the output of the Gabor filters in order to compress the data. This is done by quantising the phase information into four levels, for each possible quadrant in the complex plane. It has been shown by Oppenheim and Lim [23] that phase information, rather than amplitude information provides the most significant information within an image. Taking only the phase will allow encoding of discriminating information in the iris, while discarding redundant information such as illumination, which is represented by the amplitude component.

These four levels are represented using two bits of data, so each pixel in the normalised iris pattern corresponds to two bits of data in the iris template. A total of 2,048 bits are calculated for the template, and an equal number of masking bits are generated in order to mask out corrupted regions within the iris. This creates a compact 256-byte template, which allows for efficient storage and comparison of irises. The Daugman system makes use of polar coordinates for normalisation, therefore in polar form the filters are given as

$$H(r, \theta) = e^{-i\omega(\theta - \theta_0)} e^{-(r - r_0)^2 / \alpha_2} e^{-i(\theta - \theta_0)^2 / \beta_2} \quad (5.2)$$

where (α, β) are the same as in Equation 4.1 and (r_0, θ_0) specify the centre frequency of the filter.

The demodulation and phase Quantisation process can be represented as

$$h_{\{Re, Im\}} = \text{sgn}\{\text{Re}, \text{Im}\} \int_{\rho} \int_{\varphi} I(\rho, \varphi) e^{-i\omega(\theta - \varphi)} e^{-(r - \rho)^2 / \alpha_2} e^{-i(\theta - \varphi)^2 / \beta_2} \rho d\rho d\varphi \quad (5.3)$$

where $h_{\{Re, Im\}}$ can be regarded as a complex valued bit whose real and imaginary components are dependent on the sign of the 2D integral, and $I(\rho, \varphi)$ is the raw iris image in a dimensionless polar coordinate system. For a detailed study of 2D Gabor wavelets see [26].

5.2.3 Log-Gabor Filters

A disadvantage of the Gabor filter is that the even symmetric filter will have a DC component whenever the bandwidth is larger than one octave [20]. However, zero DC component can be obtained for any bandwidth by using a Gabor filter which is Gaussian on a logarithmic scale, this is known as the Log-Gabor filter. The frequency response of a Log-Gabor filter is given as;

$$G(f) = \exp \left(\frac{(\log(f / f_0))^2}{2(\log(\sigma / f_0))^2} \right) \quad (5.4)$$

where f_0 represents the centre frequency, and σ gives the bandwidth of the filter. Details of the Log-Gabor filter are examined by Field [20].

5.2.4 Zero-crossings of the 1D wavelet

Boles and Boashash [8] make use of 1D wavelets for encoding iris pattern data. The mother wavelet is defined as the second derivative of a smoothing function $\theta(x)$.

$$\psi(x) = \frac{d^2 \theta(x)}{dx^2} \quad (5.5)$$

The zero crossings of dyadic scales of these filters are then used to encode features. The wavelet transform of a signal $f(x)$ at scale s and position x is given by

$$\begin{aligned} W_s f(x) &= \int_{f * s} \frac{d^2 \theta(x)}{dx^2} (x) \\ &= s^2 \frac{d^2}{dx^2} (f * \theta_s)(x) \end{aligned} \quad (5.6)$$

where

$$\theta_s = (1/s)\theta(x/s)$$

$W_s f(x)$ is proportional to the second derivative of $f(x)$ smoothed by $\theta_s(x)$, and the zero crossings of the transform correspond to points of inflection in $f^* \theta_s(x)$. The motivation for this technique is that zero-crossings correspond to significant features with the iris region.

5.2.5 Haar Wavelet

Lim et al. [9] also use the wavelet transform to extract features from the iris region. Both the Gabor transform and the Haar wavelet are considered as the mother wavelet. From multi-dimensionally filtering, a feature vector with 87 dimensions is computed. Since each dimension has a real value ranging from -1.0 to +1.0, the feature vector is sign quantised so that any positive value is represented by 1, and negative value as 0. This results in a compact biometric template consisting of only 87 bits.

Lim et al. compare the use of Gabor transform and Haar wavelet transform, and show that the recognition rate of Haar wavelet transform is slightly better than Gabor transform by 0.9%.

5.2.6 Laplacian of Gaussian Filters

In order to encode features, the Wildes et al. system decomposes the iris region by application of Laplacian of Gaussian filters to the iris region image. The filters are given as

$$\nabla^2 G = -\frac{1}{\pi\sigma^4} - \frac{\rho^2}{2\sigma^6} e^{-\rho^2/2\sigma^2} \quad (5.7)$$

where σ is the standard deviation of the Gaussian and ρ is the radial distance of a point from the centre of the filter.

The filtered image is represented as a Laplacian pyramid which is able to compress the data, so that only significant data remains. Details of Laplacian Pyramids are presented by Burt and Adelson [24]. A Laplacian pyramid is constructed with four different resolution levels in order to generate a compact iris template.

4.6 Literature Review of Matching Algorithms

5.3.1 Hamming distance

The Hamming distance gives a measure of how many bits are the same between two bit patterns. Using the Hamming distance of two bit patterns, a decision can be made

as to whether the two patterns were generated from different irises or from the same one.

In comparing the bit patterns X and Y , the Hamming distance, HD , is defined as the sum of disagreeing bits (sum of the exclusive-OR between X and Y) over N , the total number of bits in the bit pattern.

$$HD = \frac{1}{N} \sum_{j=1}^N X_j (XOR) Y_j \quad (5.8)$$

$$N_{j=1}$$

Since an individual iris region contains features with high degrees of freedom, each iris region will produce a bit-pattern which is independent to that produced by another iris, on the other hand, two iris codes produced from the same iris will be highly correlated.

If two bits patterns are completely independent, such as iris templates generated from different irises, the Hamming distance between the two patterns should equal 0.5. This occurs because independence implies the two bit patterns will be totally random, so there is 0.5 chance of setting any bit to 1, and vice versa. Therefore, half of the bits will agree and half will disagree between the two patterns. If two patterns are derived from the same iris, the Hamming distance between them will be close to 0.0, since they are highly correlated and the bits should agree between the two iris codes.

The Hamming distance is the matching metric employed by Daugman, and calculation of the Hamming distance is taken only with bits that are generated from the actual iris region.

5.3.2 Weighted Euclidean Distance

The weighted Euclidean distance (WED) can be used to compare two templates, especially if the template is composed of integer values. The weighting Euclidean distance gives a measure of how similar a collection of values are between two templates. This metric is employed by Zhu et al. [11] and is specified as

$$WED(k) = \sum_{i=1}^N \frac{(f_i - f_i^{(k)})^2}{(\delta_i^{(k)})^2} \quad (5.9)$$

where f_i is the i^{th} feature of the unknown iris, and $f_i^{(k)}$ is the i^{th} feature of iris template, k , and $\delta_i^{(k)}$ is the standard deviation of the i^{th} feature in iris template k . The unknown iris template is found to match iris template k , when WED is a minimum at k .

5.3.3 Normalised Correlation

Wildes et al. make use of normalised correlation between the acquired and database representation for goodness of match. This is represented as

$$\frac{\sum_{i=1}^n \sum_{j=1}^m (p_1[i, j] - \mu_1)(p_2[i, j] - \mu_2)}{nm\sigma_1\sigma_2} \quad (5.10)$$

where p_1 and p_2 are two images of size $n \times m$, μ_1 and σ_1 are the mean and standard deviation of p_1 , and μ_2 and σ_2 are the mean and standard deviation of p_2 .

Normalised correlation is advantageous over standard correlation, since it is able to account for local variations in image intensity that corrupt the standard correlation calculation.

4.7 Implementation

5.4.1 Feature Encoding

Feature encoding was implemented by convolving the normalised iris pattern with 1D Log-Gabor wavelets. The 2D normalised pattern is broken up into a number of 1D signals, and then these 1D signals are convolved with 1D Gabor wavelets. The rows of the 2D normalised pattern are taken as the 1D signal, each row corresponds to a circular ring on the iris region. The angular direction is taken rather than the radial one, which corresponds to columns of the normalised pattern, since maximum independence occurs in the angular direction.

The intensity values at known noise areas in the normalised pattern are set to the average intensity of surrounding pixels to prevent influence of noise in the output of the filtering. The output of filtering is then phase quantised to four levels using the Daugman method [1], with each filter producing two bits of data for each phasor. The output of phase quantisation is chosen to be a grey code, so that when going from one quadrant to another, only 1 bit changes. This will minimise the number of bits disagreeing, if say two intra-class patterns are slightly misaligned and thus will provide more accurate recognition. The feature encoding process is illustrated in Figure 5.2.

The encoding process produces a bitwise template containing a number of bits of information, and a corresponding noise mask which corresponds to corrupt areas within the iris pattern, and marks bits in the template as corrupt. Since the phase information will be meaningless at regions where the amplitude is zero, these regions are also marked in the noise mask. The total number of bits in the template will be the angular resolution times the radial resolution, times 2, times the number of filters used. The number of filters, their centre frequencies and parameters of the modulating Gaussian function in order to achieve the best recognition rate will be discussed in the next chapter.

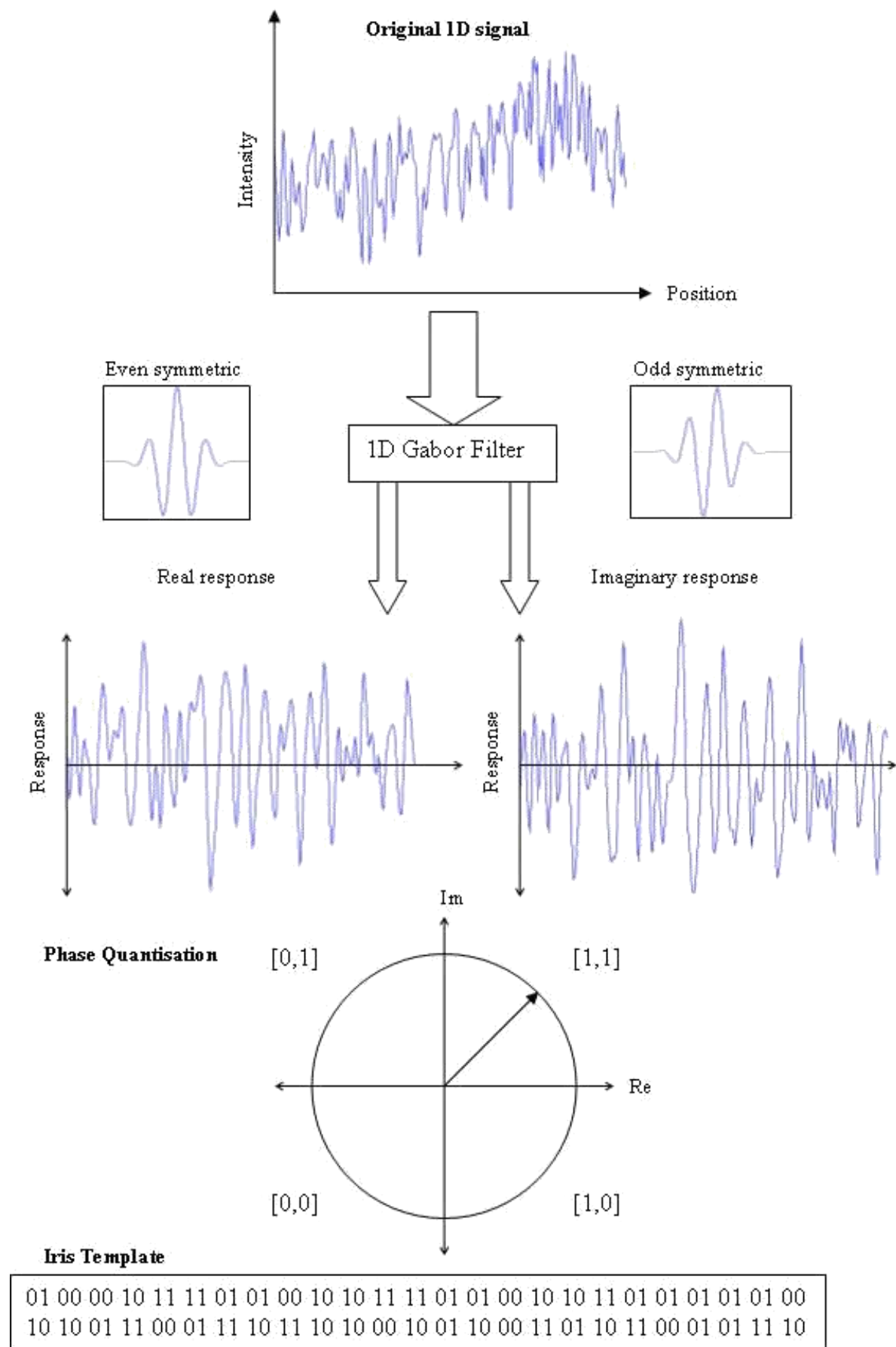


Figure 5.2 – An illustration of the feature encoding process.

5.4.2 Matching

For matching, the Hamming distance was chosen as a metric for recognition, since bit-wise comparisons were necessary. The Hamming distance algorithm employed also incorporates noise masking, so that only significant bits are used in calculating the Hamming distance between two iris templates. Now when taking the Hamming distance, only those bits in the iris pattern that corresponds to '0' bits in noise masks of both iris patterns will be used in the calculation. The Hamming distance will be calculated using only the bits generated from the true iris region, and this modified Hamming distance formula is given as

$$HD = \frac{1}{N - \sum_{k=1}^N X_{n_k} (OR) Y_{n_k}} \sum_{j=1}^N X_j (XOR) Y_j (AND) X_{n'_j} (AND) Y_{n'_j} \quad (5.11)$$

where X_j and Y_j are the two bit-wise templates to compare, X_{n_j} and Y_{n_j} are the corresponding noise masks for X_j and Y_j , and N is the number of bits represented by each template.

Although, in theory, two iris templates generated from the same iris will have a Hamming distance of 0.0, in practice this will not occur. Normalisation is not perfect, and also there will be some noise that goes undetected, so some variation will be present when comparing two intra-class iris templates.

In order to account for rotational inconsistencies, when the Hamming distance of two templates is calculated, one template is shifted left and right bit-wise and a number of Hamming distance values are calculated from successive shifts. This bit-wise shifting in the horizontal direction corresponds to rotation of the original iris region by an angle given by the angular resolution used. If an angular resolution of 180 is used, each shift will correspond to a rotation of 2 degrees in the iris region. This method is suggested by Daugman [1], and corrects for misalignments in the normalised iris pattern caused by rotational differences during imaging. From the calculated Hamming distance values, only the lowest is taken, since this corresponds to the best match between two templates.

The number of bits moved during each shift is given by two times the number of filters used, since each filter will generate two bits of information from one pixel of the normalised region. The actual number of shifts required to normalise rotational inconsistencies will be determined by the maximum angle difference between two images of the same eye, and one shift is defined as one shift to the left, followed by one shift to the right. The shifting process for one shift is illustrated in Figure 4.3.

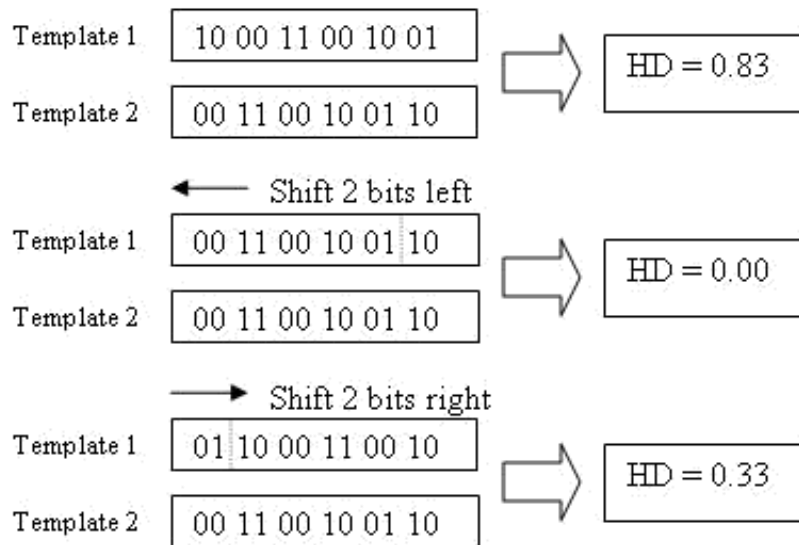


Figure 5.3 – An illustration of the shifting process. One shift is defined as one shift left, and one shift right of a reference template. In this example one filter is used to encode the templates, so only two bits are moved during a shift. The lowest Hamming distance, in this case zero, is then used since this corresponds to the best match between the two templates.

Chapter 6

SYSTEM TESTING AND PERFORMANCE EVALUATION

6.1 Overview

Software testing is conducted to verify and validate the system's functionality. In Chapter V the system requirements are outlined, in this chapter segmentation, normalization, and matching subsystems were tested and evaluated to check whether the integrated system meets these requirements. The project has achieved an iris recognition system that is fully functional. The system was tested using a database of gray scaled eye images. This chapter explains in detail the testing and performance evaluation procedure.

The mini subsystems were completed to accomplish the automated iris recognition system. The first subsystem is segmentation that extracts the iris region from the rest of the eye image. The second subsystem is normalization which eliminates dimensional inconsistencies between iris regions. MATLAB 14b is used to complete this project. It is extremely fast and flexible for the large amount of calculations that need to be performed for each iris.

6.2 TECHNICAL SPECIFICATIONS:

☐ Hardware requirements:

Name	Description
Processor	Intel or pentium4Processor
RAM	256 MB or above
Hard Disk	500 GB

☐ Software requirements:

Name	Description
O.S.	Windows
Tool	Matlab

6.3 SEGMENTATION TESTING

The CASIA database is a good tool for segmentation that is because the main for collecting the database, is to be employed for iris recognition research. The inner and the outer boundaries were extremely clear. Segmentation is a two-step process. First the pupil boundary was detected by scanning the image line by line, rows and columns, and applying an appropriate threshold. The maximum number of black pixels is the pupil diameter. Second, the iris region is segmented from an eye image using circular approximation technique. Segmentation is very important step for achieving an accurate iris recognition system. Also it is a difficult part to accomplish because the success of segmentation relay on the images used. Therefore the automatic segmentation was a great success. Over 780 out 1000 eye images were segmented correctly, the successful segmentation rate is over 78% .

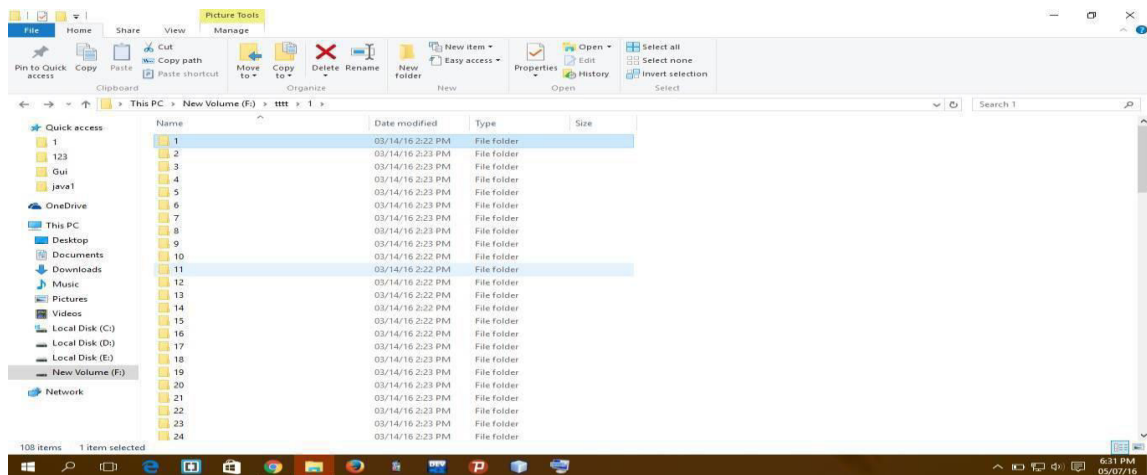


Figure 6.1:-Input Dataset (CASIA)

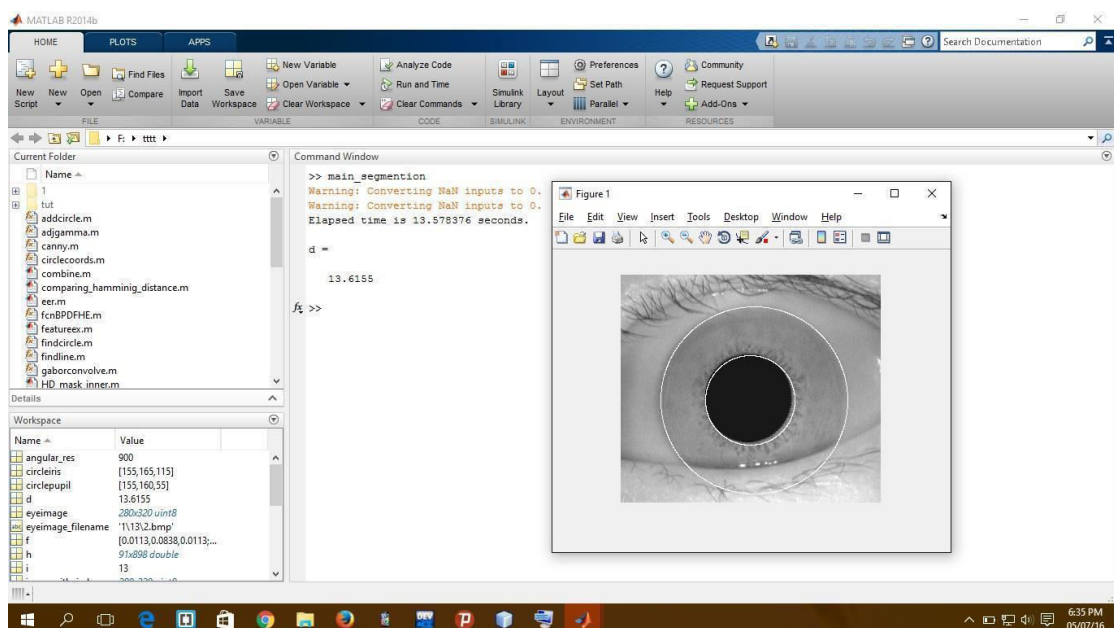


Figure 6.2:- Output of Localization Process

6.4 NORMALIZATION TESTING

Once the iris segmentation is accomplished the region was normalized. This process gives all iris images the same dimension. The Daugman rubber sheet is implemented to achieve normalization. The iris is presented as a rubber sheet, which is unwrapped into a rectangular block with constant polar dimensions. The normalization process is not able to fully reform the same pattern from images with different pupil dilation, nevertheless, it is proven to be a successful process. About 90 % of the segmented iris is normalized correctly. Figure 4.2 shows the testing and results of the normalization subsystem.

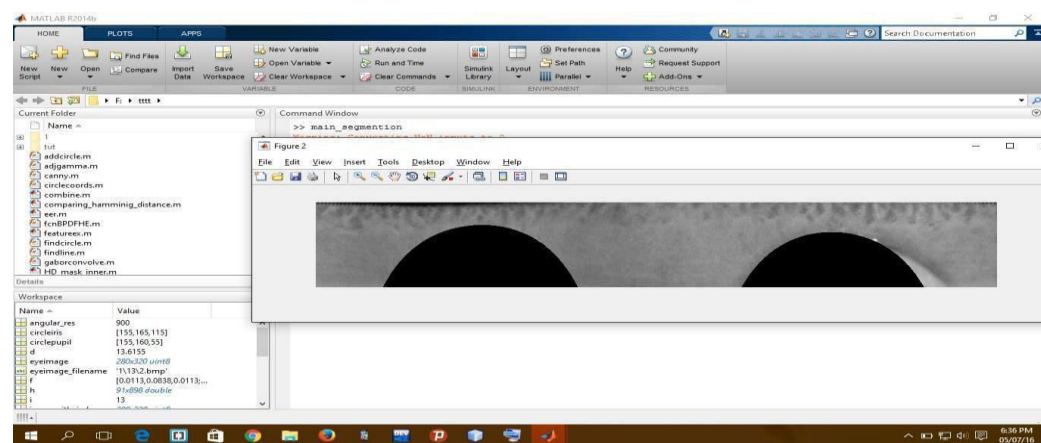


Figure 6.3:- Normalize image with Noisy part

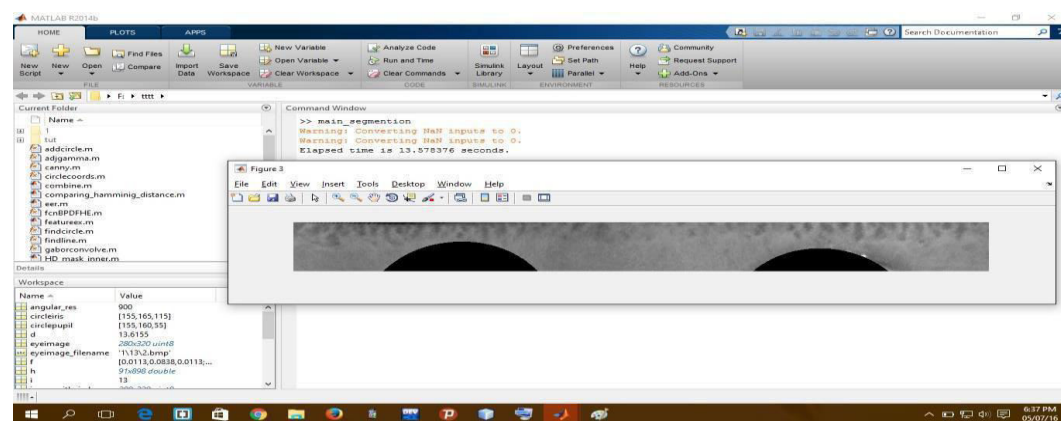


Figure 6.4:- Normalize image without Noisy part

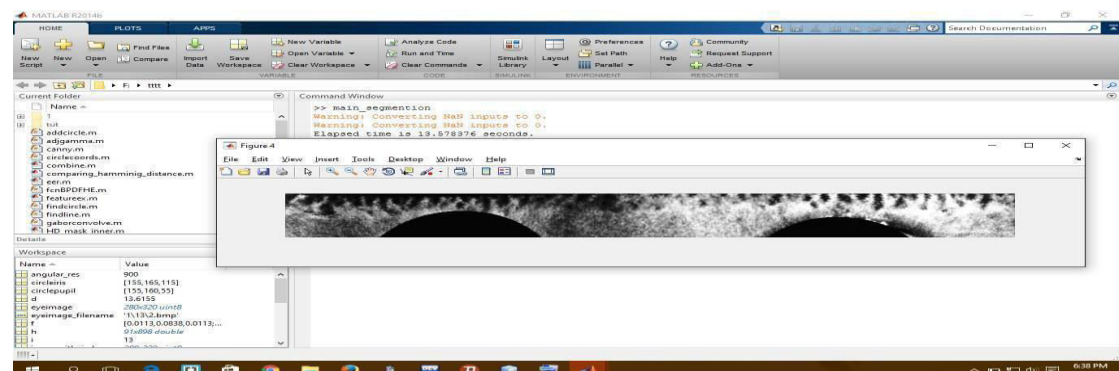


Figure 6.5:- Enhancement of Normalize image

Chapter 7

CONCLUSION AND SCOPE

7.1 Conclusion

The goal of this project is to develop an iris recognition system by designing and implementing four subsystems, namely, localization, normalization, feature extraction, and matching. The system was built following the Systems Engineering steps for designing subsystems. After testing the system, the system is fully functional, and met all functional requirements. Detailed design was done for each subsystem, and iris recognition algorithms were developed and implemented. The implementation environment for subsystems was Java. The algorithms were tested and the results were verified and validated. Systems Engineering Management Plan employed as a management foundation for the development of the system. Need analysis and need identification were accomplished for the system on the conceptual phase. In Chapter I, conceptual design for the iris recognition software system was built by analyzing the system constraints and system requirements. Chapter II covers analysis of alternatives for the system design. The proposed system was broken down into Segmentation Subsystem, Normalization Subsystem, and matching Subsystem. Maintenance and phase-out plan was accomplished for valuable system operation. After explaining the cost analysis for the system, it is expected to operate for four years with minimal changes.

Phase-out is done in the retirement period as discussed in Section 7.1. Therefore, the proposed system design satisfied the requirements and constraints. The iris recognition system will have a payout period from estimated cash flow diagram after 2.4 years.

7.2 LIMITATION

Even though, this research produced accurate results, the following issues need to be addressed: To identify a person with glasses, the reflection from glasses on the image generates failure of segmentation and recognition. To identify someone wearing colored contacted lenses, the fake iris pattern printed on the surface of the lens it creates confusion, and generate false reject or false accept results. Identifying someone with any contact lenses, the contact border can be confused by iris boundary. This confusion might result in false detection or false rejection.

7.3 FUTURE SCOPE

Our experimental results demonstrates that enhanced method for pupil extraction and five level decomposition for iris image has significantly encouraging and promising results in terms of EER and CRR. Our Feature work will include:

- ☐ Improving effectiveness in matching in terms of computational cost time.
- ☐ We are also currently working on global textural analysis with more levels of decomposition with accurate feature
- ☐ Extraction of feature from larger database similar to **Daugman's methods**.

Appendix A

System Overview

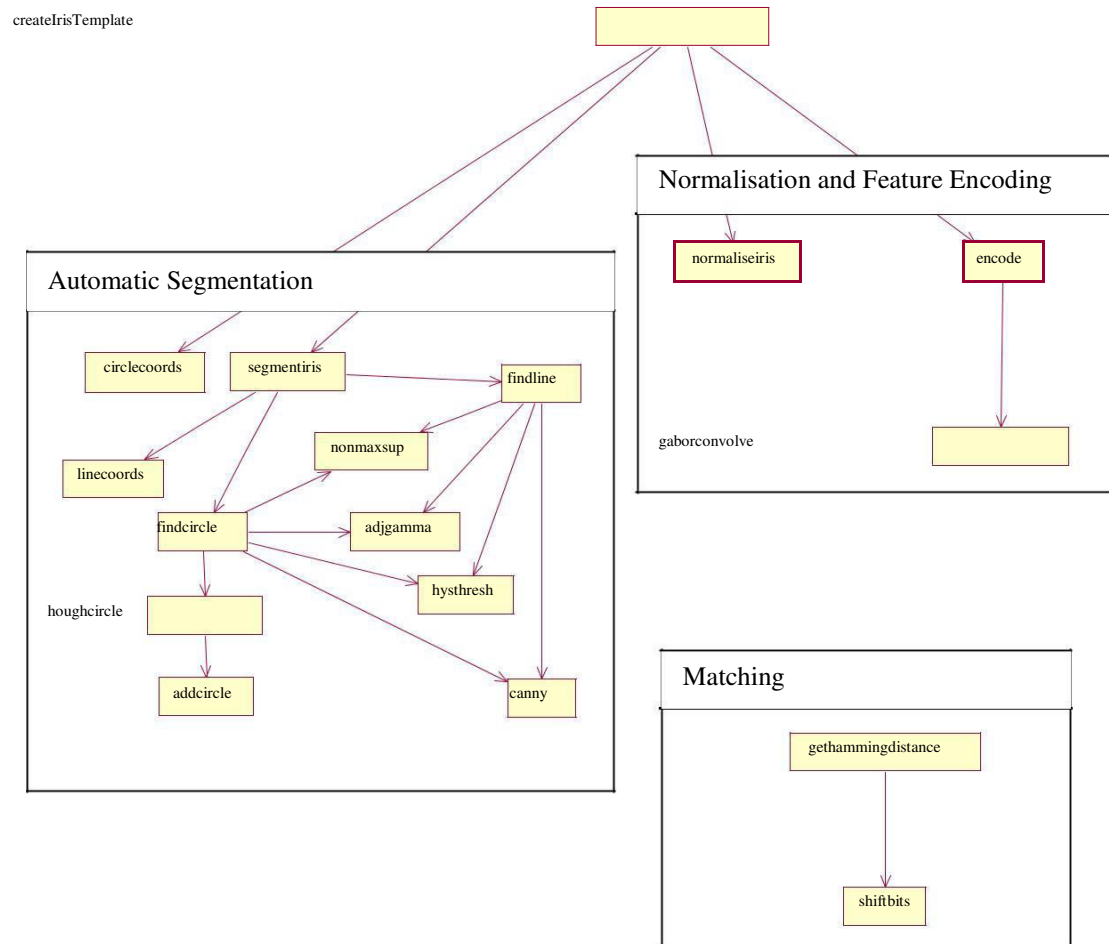


Figure B.1 – An overview of the sub-systems and MATLAB® functions that make up the iris recognition software system.

Appendix B

Detailed Experimental Results

λ_{\min}	μ_s	σ_s	μ_d	σ_d	d'	DOF
2.0	0.4522	0.0317	0.4843	0.0073	1.3910	4640
3.0	0.4162	0.0443	0.4849	0.0065	2.1716	5959
4.0	0.3731	0.0553	0.4823	0.0079	2.7676	3951
5.0	0.3394	0.0598	0.4808	0.0088	3.3091	3206
6.0	0.3127	0.0631	0.4786	0.0100	3.6696	2475
7.0	0.2914	0.0641	0.4762	0.0123	4.0080	1695
8.0	0.2754	0.0626	0.4742	0.0139	4.3874	1313
9.0	0.2658	0.0613	0.4737	0.0148	4.6636	1131
10.0	0.2605	0.0605	0.4738	0.0154	4.8299	1048
11.0	0.2569	0.0613	0.4742	0.0162	4.8445	951
12.0	0.2531	0.0617	0.4743	0.0175	4.8728	814
13.0	0.2495	0.0623	0.4743	0.0197	4.8643	644
14.0	0.2465	0.0628	0.4737	0.0216	4.8385	532
15.0	0.2469	0.0633	0.4734	0.0233	4.7475	460
16.0	0.2481	0.0632	0.4734	0.0248	4.6945	405
17.0	0.2490	0.0654	0.4734	0.0263	4.5029	360
18.0	0.2485	0.0664	0.4728	0.0281	4.4026	317
19.0	0.2485	0.0678	0.4722	0.0297	4.2756	282
20.0	0.2481	0.0683	0.4718	0.0312	4.2148	255
21.0	0.2462	0.0683	0.4713	0.0326	4.2064	234
22.0	0.2450	0.0693	0.4706	0.0339	4.1345	217
23.0	0.2439	0.0700	0.4700	0.0352	4.0804	201
24.0	0.2430	0.0719	0.4694	0.0365	3.9712	187
25.0	0.2432	0.0733	0.4688	0.0380	3.8640	173

Table C.1 – Decidability of the ‘LEI-a’ data set with various centre wavelengths using just one filter, with sigmaOnF of 0.75 with a template size of 20x240, and 3 shifts.

λ_{\min}	μ_s	σ_s	μ_d	σ_d	d'	DOF
2.0	0.4100	0.0432	0.4867	0.0051	2.4932	9477
3.0	0.3747	0.0490	0.4859	0.0056	3.1858	7940
4.0	0.3439	0.0542	0.4846	0.0065	3.6443	5965
5.0	0.3201	0.0575	0.4836	0.0076	3.9840	4337
6.0	0.3002	0.0582	0.4827	0.0086	4.3870	3342
7.0	0.2867	0.0587	0.4823	0.0096	4.6530	2712
8.0	0.2754	0.0590	0.4820	0.0104	4.8802	2324
9.0	0.2663	0.0587	0.4817	0.0111	5.1018	2021
10.0	0.2590	0.0590	0.4815	0.0121	5.2284	1703
11.0	0.2531	0.0587	0.4813	0.0131	5.3653	1460
12.0	0.2487	0.0589	0.4810	0.0140	5.4292	1272
13.0	0.2448	0.0601	0.4806	0.0150	5.3850	1126
14.0	0.2419	0.0604	0.4802	0.0157	5.4015	1011
15.0	0.2394	0.0612	0.4798	0.0167	5.3588	897
16.0	0.2372	0.0610	0.4794	0.0179	5.3854	781
17.0	0.2357	0.0615	0.4789	0.0190	5.3460	691
18.0	0.2348	0.0618	0.4784	0.0202	5.3015	613
19.0	0.2335	0.0626	0.4780	0.0214	5.2262	547
20.0	0.2323	0.0631	0.4775	0.0225	5.1756	492
21.0	0.2313	0.0634	0.4770	0.0238	5.1299	442
22.0	0.2309	0.0640	0.4765	0.0249	5.0560	404
23.0	0.2304	0.0646	0.4759	0.0260	4.9833	369
24.0	0.2300	0.0650	0.4754	0.0272	4.9263	338
25.0	0.2296	0.0651	0.4750	0.0284	4.8853	310

Table C.2 – Decidability of the ‘LEI-a’ data set with various centre wavelengths using just one filter, with sigmaOnF of 0.5 with a template size of 20x240, and 3 shifts.

λ_{\min}	μ_s	σ_s	μ_d	σ_d	d'	DOF
2.0	0.3514	0.0502	0.4856	0.0061	3.7525	6721
3.0	0.3278	0.0522	0.4847	0.0070	4.2151	5042
4.0	0.3103	0.0534	0.4842	0.0081	4.5479	3818
5.0	0.2966	0.0543	0.4836	0.0092	4.8023	2965
6.0	0.2866	0.0554	0.4831	0.0101	4.9345	2437
7.0	0.2777	0.0558	0.4825	0.0111	5.0946	2016
8.0	0.2708	0.0565	0.4820	0.0122	5.1697	1689
9.0	0.2647	0.0568	0.4813	0.0132	5.2570	1443
10.0	0.2596	0.0572	0.4810	0.0145	5.3077	1193
11.0	0.2549	0.0574	0.4804	0.0155	5.3632	1033
12.0	0.2514	0.0572	0.4799	0.0168	5.4180	880

13.0	0.2485	0.0575	0.4794	0.0181	5.4138	759
14.0	0.2461	0.0579	0.4790	0.0195	5.3884	657
15.0	0.2442	0.0588	0.4785	0.0208	5.3115	576
16.0	0.2422	0.0592	0.4781	0.0222	5.2713	504
17.0	0.2409	0.0597	0.4776	0.0236	5.2153	446
18.0	0.2400	0.0603	0.4767	0.0251	5.1334	396
19.0	0.2390	0.0612	0.4765	0.0266	5.0355	351
20.0	0.2382	0.0622	0.4760	0.0281	4.9283	316
21.0	0.2380	0.0627	0.4755	0.0296	4.8452	285
22.0	0.2377	0.0632	0.4748	0.0310	4.7623	259
23.0	0.2378	0.0636	0.4745	0.0326	4.6827	235
24.0	0.2383	0.0643	0.4740	0.0340	4.5857	216
25.0	0.2383	0.0651	0.4734	0.0355	4.4823	198

Table C.3 - Decidability of the ‘LEI-a’ data set with various centre wavelengths using just one filter, with sigmaOnF of 0.3 with a template size of 20x240, and 3 shifts.

λ_{min}	μ_s	σ_s	μ_d	σ_d	d'	DOF
4.0	0.4301	0.0358	0.4785	0.0066	1.8787	5776
8.0	0.3453	0.0431	0.4731	0.0097	4.0938	2647
12.0	0.3109	0.0399	0.4759	0.0093	5.6981	2914
13.0	0.3053	0.0399	0.4750	0.0099	5.8397	2550
14.0	0.3006	0.0398	0.4742	0.0106	5.9642	2235
15.0	0.2966	0.0396	0.4734	0.0113	6.0674	1962
16.0	0.2931	0.0396	0.4725	0.0120	6.1344	1723
17.0	0.2903	0.0395	0.4715	0.0128	6.1736	1518
18.0	0.2877	0.0394	0.4705	0.0136	6.1987	1342
19.0	0.2853	0.0396	0.4694	0.0145	6.1748	1186
20.0	0.2832	0.0399	0.4683	0.0154	6.1206	1045
21.0	0.2812	0.0401	0.4671	0.0164	6.0660	925

Table C.4 – Different filter parameters using ‘CASIA-a’ with one filter with sigmaonf of 0.5, template size 20x240, 8 shifts L & R

#Shifts L&R	μ_s	σ_s	μ_d	σ_d	d'	DOF
0	0.3047	0.0914	0.4992	0.0184	2.9489	738
1	0.2654	0.0706	0.4918	0.0173	4.4019	835
2	0.2511	0.0608	0.4856	0.0153	5.2860	1060
3	0.2487	0.0589	0.4810	0.0140	5.4292	1272
4	0.2487	0.0589	0.4777	0.0132	5.3679	1427
5	0.2487	0.0589	0.4750	0.0128	5.3148	1533
6	0.2487	0.0589	0.4730	0.0123	5.2750	1640

7	0.2487	0.0589	0.4716	0.0120	5.2479	1739
8	0.2487	0.0589	0.4705	0.0117	5.2276	1817
9	0.2487	0.0589	0.4697	0.0116	5.2090	1851
10	0.2487	0.0589	0.4690	0.0115	5.1933	1879

Table C.5 – Effect of shifts with the ‘LEI-a’ data set.

#Shifts L&R	μ_s	σ_s	μ_d	σ_d	d'	DOF
0	0.3602	0.0731	0.4993	0.0153	2.6345	1061
1	0.3352	0.0611	0.4930	0.0142	3.5576	1240
2	0.3213	0.0520	0.4888	0.0128	4.4253	1524
3	0.3184	0.0502	0.4849	0.0112	4.5780	1991
4	0.3150	0.0431	0.4828	0.0108	5.3473	2152
5	0.3145	0.0427	0.4803	0.0099	5.3494	2547
6	0.3134	0.0403	0.4793	0.0096	5.6652	2684
7	0.3133	0.0399	0.4784	0.0094	5.6959	2824
8	0.3130	0.0397	0.4771	0.0091	5.7043	2989
9	0.3130	0.0397	0.4713	0.0090	5.4994	3076
10	0.3130	0.0397	0.4757	0.0089	5.6607	3124

Table C.6 – Effect of shifts with the ‘CASIA-a’ data set.

Bibliography

- [1] S.Sangeetha S.Balgani, K.Nathiya "A new application of multimodal biometrics supporting a highly secured and authenticated service in automated teller machine (ATM)", International Journal of communications and Engineering, Vol.5, 2012.
- [2] S. Pravinthraja, K. mamaheswari," Multimodal Biometrics for Improving Automatic Teller Machine Security", International Journal of Advances in Image processing, Vol 1, 2011.
- [3] B.Shantini, S.Swamynathan, "Privacy protected multimodal biometric based group authentication scheme for ATM", Information Technology Journal, Vol 12, 2013.
- [4] Junying Gan, Peng Wang, "A novel model for face recognition", International Conference on System Science and Engineering (ICSSE), 2011.
- [5] C. Nastar and M. Mitschke, "Real time face recognition using feature combination," in Third IEEE International Conference on Automatic Face and Gesture Recognition. Nara, Japan, 1998.
- [6] S. Gong, S. J. McKenna, and A. Psarrou., Dynamic Vision: From Images to Face Recognition: Imperial College press (World Scientific Publishing Company).
- [7] T. Jebara, "3D Pose Estimation and Normalization for Face Recognition," Center for Intelligent Machines, McGill University, And Undergraduate Thesis May, 1996.
- [8] P. J. Phillips, H. Wechsler, J.Huang, and P. J. Rauss, "The FERET database and evaluation procedure for face-recognition algorithm," Image and Vision Computing, Vol.16, 1998.
- [9] D. Blackburn, J. Bone, and P. J. Phillips, "Face recognition vendor test 2000," Defense Advanced Research Projects Agency, Arlington, VA, Technical report A269514, February 16, 2001.
- [10] P. J. Phillips, P. Grother, R. J. Micheals, D. M. Blackburn, E. Tabassi, and J. M. Bone, "Face Recognition Vendor Test (FRVT 2002)," National Institute of Standards and Technology, Evaluation report IR 6965, March, 2003.
- [11] K. Messer, J. Kittler, M. Sadeghi, M. Hamouz, A. Kostin, F. Cardinaux, S. Marcel, S. Bengio, C. Sanderson, J. Czyz, L. Vandendorpe, C. McCool, S. Lowther, S. Sridharan, V. Chandran, R. P. Palacios, E. Vidal, L. Bai, L. Shen, Y. Wang, Y.-H. Chiang, H.-C. Liu, Y.-P. Hung, A. Heinrichs, M. Müller, A. Tewes, C. v. d. Malsburg, R. P. Würtz, Z. Wang, F. Xue, Y. Ma, Q. Yang, C. Fang, X. Ding, S. Lucey, R. Goss, H. Schneiderman, N. Poh, and Y. Rodriguez, "Face Authentication Test on the BANCA Database," in 17th International Conference on Pattern Recognition, Vol.4. Cambridge, UK, 2004.
- [12] X. Q. Ding and C. Fang, "Discussions on some problems in face recognition," in Advances In Biometric Person Authentication, Proceedings, Vol. 3338, Lecture Notes In Computer Science: Springer Berlin / Heidelberg, 2004.
- [13] P. J. Phillips, H. Moon, P. J. Rauss, and S. A. Rizvi, "The FERET Evaluation Methodology for Face Recognition Algorithms," IEEE Transactions on Pattern Analysis and Machine.
- [14] W. Zhao, R. Chellappa, P. Phillips, and A. Rosenfeld, "Face Recognition: A Literature Survey," ACM Computing Surveys, Vol.35, 2003.
- [15] Rabia jafri and Hamid R.Arabina,"A Survey of Face Recognition Techniques," Journal of Information Processing Systems, Vol.5, No.2, June 2009 Dept. of Computer Science, University of Georgia, Athens, Georgia, U.S.A.
- [16] Krishna Dharavath, F. A. Talukdar, R. H. Laskar ,," Study on Biometric Authentication Systems, Challenges and Future Trends: A Review", IEEE International Conference on Computational Intelligence,2013 National Institute of Technology Silchar, India.
- [17] Tiwalade O. Majekodunmi, Francis E. Idachaba," A Review of the Fingerprint, Speaker Recognition, Face Recognition and Iris Recognition Based Biometric Identification Technologies", Proceedings of the World Congress on Engineering 2011 Vol II WCE 2011, July 6 - 8, 2011, London, U.K.
- [18] Ruud M. Bolle, Jonathan H. Connell, Sharath Pankanti, Nalini K. Ratha, and Andrew W. Senior, Guide to Biometrics. Springer Science Business Media, Inc, NY 10013, USA, 2004.
- [19] Julian Ashbourn, Practical Biometrics: From Aspiration to Implementation. Springer-Verlag London, 2004.
- [20] Ms. C.B. Tatepamulwar, Dr. V. P. Pawar," Comparison of Biometric Trends Based on Different Criteria", Asian Journal of Management Sciences, 2014.
- [21] Marcosfaundez-Zanuy", Biometric Security Technology, IEEE A&E Systems Magazine VOL. 21, JUNE 2006 Escola Universitaria Politecnica' de Mataro' spain.
- [22] Nishit Shah,Pravin Shrinath,"Iris Recognition System-A Review", International Journal of Computer and Information Technology(ISSN: 2279-0764)Volume 03-Issue 02,March 2014.
- [23] Gursimarpreet Kaur,Dr.Chander Kant Verma", Comparative Analysis of Biometric Modalities",IJARCSSE April-2014.
- [24] Jain, A. K.; Ross, A. & Pankanti, S., "Biometrics: A Tool for Information Security," IEEE Transactions on Infor-mation Forensics And Security, Vol. 1, 2006.
- [25] Knowledge-Based Intelligent Information and Engineering Systems: 8th International Conference, KES 2004, Wellington, New Zealand, September 20-25,2004.
- [26] (2010, August 10). Fingerprint recognition- Wikipedia, the free Encyclopedia [Online].Available: http://en.wikipedia.org/wiki/Fingerprint_recognition .
- [27] Y. Zhu, T. Tan, and Y. Wang (2000). "Biometric Personal Identification Based on Iris Patterns", Proceedings of the 15th International Conference on Pattern Recognition, Vol. 2.
- [28] L.Ma, Y. Wang, and T. Tan (2002). "Iris recognition using circular symmetric filters", International Conference on Pattern Recognition, Vol.2.
- [29] J. Huang, Y. Wang, T. Tan, and J. Cui (2004). "A New Iris Segmentation Method for Recognition", Proceedings of the 17th International Conference on Pattern Recognition.
- [30] Richard Yew Fatt Ng, Yong Haur Tav, and Kai Ming Mok, "A Review of Iris Recognition Algorithms,"Computer Vision and Intelligent System(CVIS) Group University Tunku abdul rahman, Malaysia, 2008 IEEE.
- [31] Dr. S.Ravi, Dattatreya P. Mankame,"Multimodal Biometrie Approach Using FingerPrint,Face and Enhanced Iris Features Recognition," 2013 IEEE.
- [32] Himanshu Srivastava,"A Comparison Based Study On Biometrics For Human Recognition," IOSR Journal of Computer Engineering (IOSR-JCE),Volume 15,Oct 2013.